Supporting Information

A family of thienyl-bis-salophen Zn(II) complexes for enhancing photoconductance in hybrid materials including platinum ultra-small nanoparticles

Melissa Dumartin [a], Adeline Pham [b], Nathalie Saffon-Merceron [c], Marine Tassé [d], Simon Tricard [b], Claire Kammerer [a] and Jacques Bonvoisin [a*]

a) CEMES, CNRS-UPR 8011, Université de Toulouse, 29 rue Jeanne Marvig, - 31055 Toulouse, France

b) Laboratoire de Physique et Chimie des Nano-Objets, INSA, CNRS-UMR5215, Université de Toulouse, 135 Avenue de Rangueil, 31077 Toulouse, France

c) Université de Toulouse, Institut de Chimie de Toulouse, ICT UAR 2599, 118 route de Narbonne, 31062 Toulouse, France

d) Laboratoire de Chimie de Coordination, CNRS-UPR8241, Université de Toulouse, 205 route de Narbonne, 31077 Toulouse, France

Table of contents

I. Synthesis and characterization of molecular targets

General methods

All chemicals and solvents were purchased from Aldrich, VWR, ABCR, TCI, Acros and Alfa Aesar and used as received. All reactions were carried out using standard Schlenk techniques under an argon atmosphere. Column chromatography was carried out on 230-400 mesh silica gel (Aldrich). Thin layer chromatography (TLC) was performed on pre-coated aluminum-backed silica gel 60 UV254 plates (Macherey–Nagel) with visualization effected using ultraviolet irradiation (λ = 254 or 366 nm).

NMR spectroscopy, mass spectrometry, X-ray diffraction and elemental analysis were performed by the appropriate services of the Toulouse Institute of Chemistry (ICT – UAR 2599).

^{1}H-NMR spectra were recorded on an Avance 300 MHz (probe 5 mm BBO BB-1H Z-GRD), Bruker Avance III HD 500 MHz (cryoprobe Prodigy 5mm BBO, ^{1}H ATMA) and Avance 500 MHz (cryoprobe 5mm ^{1}H, ^{13}C) spectrometers. Full assignments of ^{1}H and ^{13}C NMR spectra were made with the assistance of COSY, HMBC, HSQC and NOESY spectra. Residual solvent signals were used as internal references; chemical shifts (δ) are reported in ppm; coupling constants (*J*) are given in Hz; the following abbreviations have been used to describe the signals: singlet (s), broad singlet (br. s), doublet (d), triplet (t), multiplet (m). For solubility reasons, some of the bis-salophen NMR spectra were recorded in a mixture of DMSO-d_6 and tetrabutylammonium acetate (TBA Acetate) salt. We believe that the acetate anion increases the solubility of the bis-salophen by coordinating on the zinc atoms, thus preventing the stacking.

High-resolution mass spectra (HRMS) were performed with a Waters MALDI micro MX spectrometer for matrix-assisted laser desorption ionization (MALDI) (matrix: *trans*-2-[3-(4-*tert*-butylphenyl)-2-methyl-2-propenylidene]malononitrile DCTB; λ= 337 nm).

Complexes were considered with various transition metals, such as Zn^{2+}, Pd^{2+}, and Pt^{2+}. Pt^{2+} was eliminated in order to easily differentiate the complexes from the Pt nanoparticles in SEM-EDX. Syntheses with Pd^{2+} proved unsuccessful. We therefore focused on Zn^{2+} complexes for this study.

The crystal data of compounds **8**, **12**, **13**, **16** and **18** were collected using MoKα radiation (wavelength=0.71073 Å) on a Bruker–AXS Quazar APEX II diffractometer using a 30W air–cooled microfocus source (ImS) with focusing multilayer optics (**8**, **13** and **16**) and on a Bruker–AXS D8–Venture diffractometer equipped with a Photon III–C14 detector (**12** and **18**). Phi and omega– scans were used. Crystals were mounted in inert oil and crystal structure determinations were affected at 193 K. The data were integrated with SAINT, [1] and an empirical absorption correction with SADABS was applied. [2] The structures were solved using intrinsic phasing method (ShelXT) [3] and refined using the least–squares method on F^2 (ShelXL). [4] All non–H atoms were refined with anisotropic displacement parameters. The H atoms were refined isotropically at calculated positions using a riding model. In most structures, some parts (especially the solvent molecules and the thiophene groups) were disordered. Several restraints (SAME, ISOR, SIMU, DELU, DFIX, DANG) and equal xyz and U_{ij} constraints (EXYZ and EADP) (**5**) were applied to refine some moieties of the molecules and to avoid the collapse of the structures during the least–squares refinement by the large anisotropic displacement parameters. In structures **16** and **18**, some residual electron density were difficult to modelize and therefore, the SQUEEZE function of PLATON [5] was used to eliminate the contribution of the electron density in the solvent region from the intensity data, and the solvent–free model was employed for the final refinement. X–ray crystallographic data have been deposited in the Cambridge Crystallographic Data Centre (http://www.ccdc.cam.ac.uk/) with reference numbers: CCDC–2404730 (**8**), CCDC–2404731 (**12**), CCDC–2404732 (**13**), CCDC–2404733 (**16**) and CCDC–2404734 (**18**). These data can be obtained free of charge from https://www.ccdc.cam.ac.uk/structures/ or from the

Cambridge Crystallographic Data Centre, 12 Union Road, Cambridge CB2 1EZ, UK; tel: + 44 (0)1223 336408; fax: + 44 (0)1223336033; or e–mail: deposit@ccdc.cam.ac.uk.

Synthetic protocols and characterization

Bis-salophen Zn(II) complex **3**

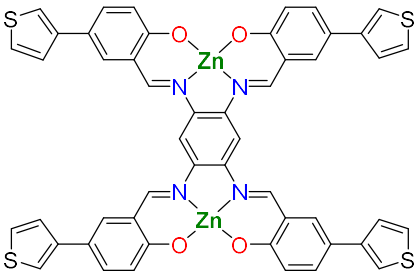

3

$C_{50}H_{30}N_4O_4S_4Zn_2$

M= 1009.81 g.mol^{-1}

Under inert atmosphere, 1,2,4,5-benzenetetramine tetrahydrochloride (0.06 mmol, 17 mg, 1 equiv.) and zinc diacetate dihydrate (0.24 mmol, 54 mg, 4 equiv.) were dispersed in DMSO (2.6 mL) to afford a dark red solution. After stirring for a few minutes, the 2-hydroxy-5-(thiophen-3-yl)benzaldehyde [6] (0.24 mmol, 50 mg, 4 equiv.) dissolved in 1 mL of DMSO was added to the dark red solution and the mixture was stirred at 60 °C for 48 h. After 48 h, an abundant orange-red precipitate was obtained. The compound was collected by filtration and washed respectively with MeOH (2 x 10 mL) and diethyl ether (2 x 10 mL). After drying in vacuo, complex **3** was obtained as a burgundy red solid with a 65% yield.

^{1}H NMR (500 MHz, DMSO-d$_6$ + TBA Acetate, 25 °C): δ = 9.17 (br. s, 4H), 8.30 (br. s, 2H), 7.81 (br. s, 4H), 7.68-7.45 (br. m, 16H) and 6.72-6.60 (br. m, 4H). Signals are very broad due to limited solubility, despite the addition of tetrabutylammonium acetate.

^{13}C NMR (126 MHz, DMSO-d$_6$ + TBA Acetate, 25 °C): δ = 172.3 (Cq), 162.0 (CH), 141.9 (Cq), 139.6 (Cq), 133.0 (CH), 132.0 (CH), 126.4 (CH), 125.7 (CH), 123.6 (CH), 119. 7 (Cq), 119.5 (Cq), 116.5 (CH) and 103.7 (CH).

HRMS (MALDI): for $C_{50}H_{30}N_4O_4NaS_4Zn_2$ M+Na$^+$ = 1028.9631 (calculated) / M+Na$^+$ = 1028.9677 (found)

EA: for $C_{50}H_{30}N_4O_4S_4Zn_2.4H_2O$, calculated: %C 55.51, %H 3.54, %N 5.18 / found (average on two trials): %C 55.15, %H 3.015, %N 5.24

Bis-salophen Zn(II) complex **5**

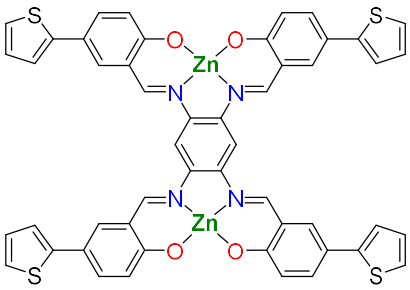

5

$C_{50}H_{30}N_4O_4S_4Zn_2$

M= 1009.81 g.mol^{-1}

Under inert atmosphere, 1,2,4,5-benzenetetramine tetrahydrochloride (0.06 mmol, 17 mg, 1 equiv.) and zinc diacetate dihydrate (0.24 mmol, 54 mg, 4 equiv.) were dispersed in DMSO (2.6 mL) to afford a dark red solution. After stirring for a few minutes, the 2-hydroxy-5-(thiophen-2-yl)benzaldehyde [7] (0.24 mmol, 50 mg, 4 equiv.) dissolved in 1 mL of DMSO was added to the dark red solution and the mixture was stirred at 60 °C for 48 h. After 48 h, an abundant red precipitate was obtained. The compound was collected by filtration and washed respectively with MeOH (2 x 10 mL) and diethyl ether (2 x 10 mL). After drying in vacuo, complex **5** was obtained as a burgundy red solid with a 65% yield.

^{1}H NMR (500 MHz, DMSO-d$_6$ + TBA Acetate, 25 °C): δ = 9.13 (br. s, 4H), 8.31 (br. s, 2H), 7.72 (br. s, 4H), 7.54 (br. d, *J*=8.8 Hz, 4H), 7.35 (dd, *J*=5.0, 1.2 Hz, 4H), 7.27 (br. m, 4H), 7.08 (dd, *J*=5.1, 3.5 Hz, 4H) and 6.68 (br. d, *J*=8.8 Hz, 4H). Some signals are broad due to limited solubility, despite the addition of tetrabutylammonium acetate.

^{13}C NMR (126 MHz, DMSO-d$_6$ + TBA Acetate, 25 °C): δ = 172.7 (Cq), 161.7 (CH), 144.7 (Cq), 139.7 (Cq), 132.4 (CH), 131.3 (CH), 128.2(CH), 123.9 (CH), 122.4 (CH), 120.3 (CH), 119.6 (Cq), 118.2 (Cq) and 104.0 (CH).

HRMS (MALDI): for $C_{50}H_{30}N_4NaO_4S_4Zn_2$ M+Na$^+$ = 1028.9631 (calculated) / M+Na$^+$ = 1028.9695 (found)

EA : for $C_{50}H_{30}N_4O_4S_4Zn_2.3H_2O$, calculated: %C 56.45, %H 3.41, %N 5.27 / found: %C 56.20, %H 3.04, %N 5.30

3-(*tert*-butyl)-2-hydroxy-5-(thiophen-3-yl)benzaldehyde (**7**)

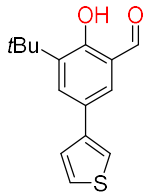

7

$C_{15}H_{16}O_2S$

M= 260.35 g.mol^{-1}

Under inert atmosphere, $Pd(PPh_3)_4$ (0.1 mmol, 116 mg, 10 mol%) was added to a stirred solution of 3-(*tert*-butyl)-2-hydroxy-5-iodobenzaldehyde (1 mmol, 300 mg, 1 equiv.), 3-thienylboronic acid (1.2 mmol, 152 mg, 1.2 equiv.), K_2CO_3 (2.5 mmol, 341 mg, 2.5 equiv.) in degassed toluene (5 mL), ethanol (1 mL) and water (0.25 mL). After stirring the reaction mixture at room temperature for 20 min, it was slowly heated to 80 °C for 48 h. After completion of the reaction (TLC monitoring) the solvents were removed under reduced pressure. The reaction mixture was dispersed in DCM (100 mL) and a solution of 5% HCl in water (20 mL) added. The organic layer was then separated, washed with brine (20 mL), dried over magnesium sulfate and evaporated under reduced pressure. The crude compound was then purified by silica gel chromatography (cyclohexane / ethyl acetate). The pure compound **7** was isolated as a pale yellow oil with a 80% yield.

Rf=0.8 (SiO_2, 80% cyclohexane + 20% ethyl acetate)

^{1}H NMR (500 MHz, CD_2Cl_2, 25 °C): δ = 11.81 (d, *J*=0.6 Hz, 1H), 9.94 (s, 1H), 7.80 (dd, *J*=2.3, 0.6 Hz, 1H), 7.64 (d, *J*=2.3 Hz, 1H), 7.45-7.43 (m, 2H), 7.40-7.39 (m, 1H) and 1.47 (s, 9H).

^{13}C NMR (126 MHz, CD_2Cl_2, 25 °C): δ = 197.9 (CH), 160.7 (Cq), 141.6 (Cq), 139.0 (Cq), 132.9 (CH), 129.7 (CH), 127.8 (Cq), 127.0 (CH), 126.4 (CH), 121.1 (Cq), 120.0 (CH), 35.3 (Cq) and 29.4 (CH_3).

HRMS (DCI): for $C_{15}H_{17}O_2S$ MH^+ = 261.0949 (calculated) / MH^+ = 261.0945 (found)

Tetra-Schiff base **8**

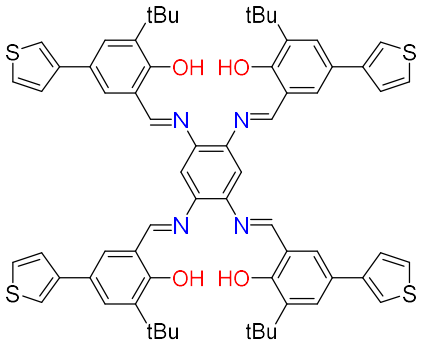

8

$C_{66}H_{66}N_4O_4S_4$

M= 1107.52 g.mol^{-1}

Under inert atmosphere, to a solution of 1,2,4,5-benzenetetramine tetrahydrochloride (25 mg, 0.09 mmol, 1 equiv.) in 3.8 mL of anhydrous methanol was added 3-(*tert*-butyl)-2-hydroxy-5-(thiophen-3-yl)benzaldehyde **7** (100 mg, 0.38 mmol, 4.2 equiv.). After 48 h continuously stirring at room temperature, the orange precipitate was collected by filtration and washed with anhydrous methanol (2 x 10 mL). After drying in vacuo, the pure tetra-Schiff base **8** was obtained as an orange solid with a 85% yield.

^{1}H NMR (300 MHz, CD_2Cl_2, 25 °C): δ = 13.78 (s, 4H), 8.90 (s, 4H), 7.68 (d, *J*=2.1 Hz, 4H), 7.57 (d, *J*=2.2 Hz, 4H), 7.43-7.38 (m, 12H), 7.34 (s, 2H) and 1.49 (s, 36H).

^{13}C NMR (126 MHz, CD_2Cl_2, 25 °C): δ = 165.0 (CH), 160.6 (Cq), 142.3 (Cq), 142.1 (Cq), 138.7 (Cq), 129.9 (CH), 128.8 (CH), 127.0 (Cq), 126.7 (CH), 126.5 (CH), 119.6 (Cq), 119.3 (CH), 111.3 (CH), 35.4 (Cq) and 29.5 (CH_3)

HRMS (MALDI): for $C_{66}H_{66}N_4O_4S_4$ $M^{+\bullet}$ = 1106.3967 (calculated) / $M^{+\bullet}$ = 1106.4047 (found)

Bis-salophen Zn(II) complex **9**

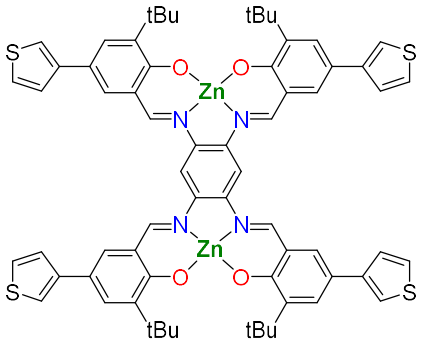

9

$C_{66}H_{62}N_4O_4S_4Zn_2$

M= 1234.25 g.mol^{-1}

Under inert atmosphere, the tetra-Schiff base **8** (65 mg, 0.059 mmol, 1 equiv.) was dispersed in 48 mL of anhydrous MeOH in a dry round bottom flask. To this suspension was added after stirring for a few minutes, a solution of zinc diacetate dihydrate (28 mg, 0.13 mmol, 2.2 equiv.) in anhydrous MeOH (2 mL). After stirring at room temperature for 4 days, the solvent was evaporated and acetonitrile added (15 mL). The solid was triturated and collected by filtration, then washed with acetonitrile (2 x 10 mL). After drying in vacuo, complex **9** was obtained as a bright red solid with a 85% yield.

^{1}H NMR (300 MHz, DMSO-d$_6$ + TBA Acetate, 25 °C): δ = 9.17 (s, 4H), 8.30 (s, 2H), 7.66 (d, *J*=2.5 Hz, 4H), 7.61 (dd, *J*= 5.0, 2.9 Hz, 4H), 7.52 (dd, *J*= 6.2, 2.7 Hz, 8H), 7.48 (d, *J*=5.0 Hz, 4H) and 1.54 (s, 36H).

^{13}C NMR (126 MHz, DMSO-d$_6$ + TBA Acetate, 25 °C): δ = 172.2 (Cq), 161.6 (CH), 142.7 (Cq), 142.0 (Cq), 139.3 (Cq), 131.2 (CH), 128.5 (CH), 126.4 (CH), 125.9 (CH), 119.5 (Cq), 118.7 (Cq), 116.5 (CH), 102.9 (CH), 35.2 (Cq) and 29.6 (CH_3).

HRMS (MALDI): for $C_{66}H_{62}N_4O_4S_4Zn_2$ $M^{+\bullet}$ = 1234.2207 (calculated) / $M^{+\bullet}$ = 1234.2296 (found)

EA: for $C_{66}H_{62}N_4O_4S_4Zn_2.4H_2O$, calculated: %C 60.68, %H 5.40, %N 4.29 / found (average on two trials): %C 60.84, %H 5.505, %N 4.765

3-(*tert*-butyl)-2-hydroxy-5-(thiophen-2-yl)benzaldehyde (**11**)

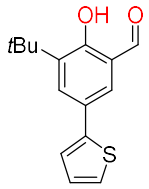

11

$C_{15}H_{16}O_2S$

M= 260.35 g.mol^{-1}

Under inert atmosphere, degassed 2-(tributylstannyl)thiophene (0.2 mL, 0.62 mmol, 1.25 equiv.) was added to a mixture of 3-(*tert*-butyl)-2-hydroxy-5-iodobenzaldehyde (0.150 g, 0.49 mmol, 1 equiv.), LiCl (63 mg, 1.48 mmol, 3 equiv.) and *trans*-dichlorobis(triphenylphosphine)palladium(II) (34 mg, 0.049 mmol, 10 mol%) in degassed dry THF (3 mL). After heating to 80 °C for 16 h, the reaction solution was concentrated then diluted with DCM (100 mL) and washed with aqueous ammonium chloride (3 × 30 mL). The organic layer was concentrated then filtered through silica, eluted with EtOAc and the solvent removed under vacuum to obtain a crude mixture, which was purified by silica gel chromatography (cyclohexane / ethyl acetate). The pure compound **11** was isolated as a bright yellow oil with a 75% yield.

Rf=0.7 (SiO_2, 90% cyclohexane + 10% ethyl acetate)

^{1}H NMR (500 MHz, CD_2Cl_2, 25 °C): δ = 11.83 (d, *J*=0.6 Hz, 1H), 9.93 (s, 1H), 7.79 (dd, *J*=2.3, 0.6 Hz, 1H), 7.65 (d, *J*=2.3 Hz, 1H), 7.30-7.27 (m, 2H), 7.10 (dd, *J*=5.1, 3.6 Hz, 1H) and 1.46 (s, 9H).

^{13}C NMR (126 MHz, CD_2Cl_2, 25 °C): δ = 197.7 (CH), 161.0 (Cq), 143.7 (Cq), 139.3 (Cq), 132.4 (CH), 129.3 (CH), 128.5 (CH), 126.4 (Cq), 124.8 (CH), 123.1 (CH), 121.1 (Cq), 35.3 (Cq) and 29.3 (CH_3).

HRMS (DCI): for $C_{15}H_{17}O_2S$ MH^+ = 261.0949 (calculated) / MH^+ = 261.0951 (found)

Tetra-Schiff base **12**

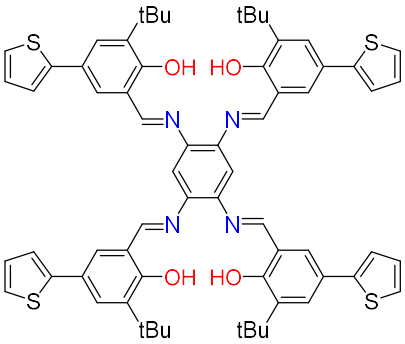

12

$C_{66}H_{66}N_4O_4S_4$

M= 1107.52 g.mol^{-1}

Under inert atmosphere, to a solution of 1,2,4,5-benzenetetramine tetrahydrochloride (25 mg, 0.09 mmol, 1 equiv.) in 3.8 mL of anhydrous methanol was added 3-(*tert*-butyl)-2-hydroxy-5-(thiophen-2-yl)benzaldehyde **11** (100 mg, 0.38 mmol, 4.2 equiv.). After 48 h continuously stirring at room temperature, the orange-brown precipitate was collected by filtration and washed with anhydrous methanol (2 x 10 mL) and acetonitrile (2 x 10 mL). After drying in vacuo, the pure tetra-Schiff base **12** was obtained with a 65% yield.

^{1}H NMR (300 MHz, DMSO-d$_6$, 25 °C): δ = 14.22 (s, 4H), 9.29 (s, 4H), 7.94 (s, 2H), 7.82 (d, *J*= 2.4 Hz, 4H), 7.66 (d, *J*= 2.4 Hz, 4H), 7.49 (d, *J*= 5.1 Hz, 4H), 7.42 (d, *J*= 3.3 Hz, 4H), 7.13 (t, *J*= 4.4 Hz, 4H) and 1.46 (s, 36H).

^{13}C NMR (126 MHz, DMSO-d$_6$, 25 °C): δ = 165.7 (CH), 159.9 (Cq), 143.2 (Cq), 141.1 (Cq), 137.7 (Cq), 128.5 (CH), 128.2 (CH), 128.0 (CH), 124.7 (CH), 124.5 (Cq), 122.6 (CH), 119.2 (Cq), 111.0 (CH), 34.7 (Cq) and 29.1 (CH_3).

HRMS (ESI): for $C_{66}H_{67}N_4O_4S_4$ MH^+ = 1107.4045 (calculated) / MH^+ = 1107.4054 (found)

Bis-salophen Zn(II) complex 13

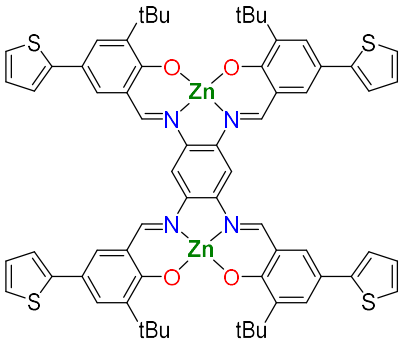

13

$C_{66}H_{62}N_4O_4S_4Zn_2$

M= 1234.25 g.mol^{-1}

Under inert atmosphere, the tetra-Schiff base **12** (47 mg, 0.038 mmol, 1 equiv.) was dispersed in 30 mL of anhydrous MeOH in a dry round bottom flask. To this suspension was added after stirring for a few minutes, a solution of zinc diacetate dihydrate (37 mg, 0.17 mmol, 4.5 equiv.) in anhydrous MeOH (1 mL). After stirring at room temperature for 4 days, the solvent was evaporated and acetonitrile added (15 mL). The solid was triturated and collected by filtration, then washed with acetonitrile (2 x 10 mL). After drying in vacuo, complex **13** was obtained as a brick red solid with a 95% yield.

^{1}H NMR (500 MHz, DMSO-d$_6$ + TBA Acetate, 25 °C): δ = 9.18 (s, 4H), 8.37 (s, 2H), 7.63 (d, *J*= 2.6 Hz, 4H), 7.47 (d, *J*= 2.6 Hz, 4H), 7.34 (dd, *J*= 5.1, 1.2 Hz, 4H), 7.23 (dd, *J*= 3.5, 1.2 Hz, 4H), 7.08 (dd, *J*= 5.1, 3.5 Hz, 4H) and 1.54 (s, 36H).

^{13}C NMR (126 MHz, DMSO-d$_6$ + TBA Acetate, 25 °C): δ = 172.5 (Cq), 161.5 (CH), 145.6 (Cq), 142.2 (Cq), 139.4 (Cq), 130.7 (CH), 128.1 (CH), 127.8 (CH), 122.3 (CH), 120.0 (CH), 119.6 (Cq), 117.1 (Cq), 103.3 (Cq), 35.2 (Cq) and 29.5 (CH_3).

HRMS (ESI): for $C_{66}H_{63}N_4O_4S_4Zn_2$ MH^+ = 1235.2285 (calculated) / MH^+ = 1235.2319 (found)

EA: for $C_{66}H_{62}N_4O_4S_4Zn_2.3H_2O$, calculated: %C 61.53, %H 5.32, %N 4.35 / found (average on two trials): %C 61.245, %H 4.955, %N 4.345

5-(*tert*-butyl)-2-hydroxy-3-(thiophen-3-yl)benzaldehyde (**15**)

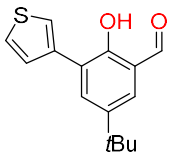

15

$C_{15}H_{16}O_2S$

M= 260.35 g.mol^{-1}

Under inert atmosphere, $Pd(PPh_3)_4$ (0.1 mmol, 116 mg, 10 mol%) was added to a stirred solution of 5-(*tert*-butyl)-2-hydroxy-3-iodobenzaldehyde (1 mmol, 300 mg, 1 equiv.), 3-thienylboronic acid (1.2 mmol, 152 mg, 1.2 equiv.), K_2CO_3 (2.5 mmol, 341 mg, 2.5 equiv.) in degassed toluene (5 mL), ethanol (1 mL) and water (0.25 mL). After stirring the reaction mixture at room temperature for 20 min, it was slowly heated to 80 °C for 48 h. After completion of the reaction (TLC monitoring) the solvents were removed under reduced pressure. The reaction mixture was dispersed in DCM (100 mL) and a solution of 5% HCl in water (20 mL) added. The organic layer was then separated, washed with brine (20 mL), dried over magnesium sulfate and evaporated under reduced pressure. The crude product was then purified by silica gel chromatography (cyclohexane / ethyl acetate). The pure compound **15** was isolated as a bright yellow solid with a 85% yield.

Rf=0.85 (SiO_2, 80% cyclohexane + 20% ethyl acetate)

^{1}H NMR (500 MHz, CD_2Cl_2, 25 °C): δ = 11.58 (d, *J*=0.6 Hz, 1H), 9.94 (s, 1H), 7.84 (dd, *J*=2.5, 0.6 Hz, 1H), 7.78 (dd, *J*=3.0, 1.3 Hz, 1H), 7.54 (d, *J*=2.5 Hz, 1H), 7.52 (dd, *J*=5.0, 1.3 Hz, 1H), 7.41 (dd, *J*=5.0, 1.3 Hz, 1H) and 1.37 (s, 9H).

^{13}C NMR (126 MHz, CD_2Cl_2, 25 °C): δ = 197.8 (CH), 157.0 (Cq), 143.2 (Cq), 137.2 (Cq), 134.6 (CH), 129.8 (CH), 128.3 (CH), 125.3 (CH), 124.6 (Cq), 124.2 (CH), 120.9 (Cq), 34.5 (Cq) and 31.5 (CH_3).

HRMS (DCI): for $C_{15}H_{17}O_2S$ MH^+ = 261.0949 (calculated) / MH^+ = 261.0950 (found)

Bis-salophen Zn(II) complex **16**

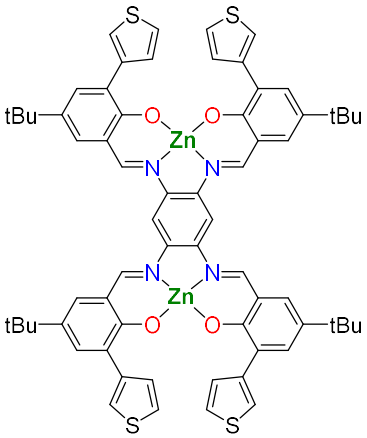

16

$C_{66}H_{62}N_4O_4S_4Zn_2$

M= 1234.25 g.mol^{-1}

Under inert atmosphere, 1,2,4,5-benzenetetramine tetrahydrochloride (0.038 mmol, 11 mg, 1 equiv.) and zinc diacetate dihydrate (0.15 mmol, 34 mg, 4 equiv.) were dispersed in DMSO (1.6 mL) to afford a dark red solution. After stirring for a few minutes, the 5-(*tert*-butyl)-2-hydroxy-3-(thiophen-3-yl)benzaldehyde **15** (0.15 mmol, 40 mg, 4 equiv.) was dissolved in 0.6 mL of DMSO and added to the dark red solution. The mixture was stirred at 60 °C for 48 h. Upon completion of the reaction (TLC monitoring), water was added (20 mL) in order to precipitate the product, which was collected by filtration and washed respectively with methanol and diethyl ether. After drying in vacuo, complex **16** was obtained as a bright red solid with a 80% yield.

^{1}H NMR (500 MHz, DMSO-d_6, 25 °C): δ = 9.28 (s, 4H), 8.57 (d, *J*=3.1 Hz, 4H), 8.45 (s, 2H), 7.84 (m, 8H), 7.58 (dd, *J*=5.0, 3.0 Hz, 4H), 7.49 (d, *J*=2.7 Hz, 4H) and 1.39 (s, 36H).

^{13}C NMR (126 MHz, DMSO-d_6, 25 °C): δ = 168.1 (Cq), 163.5 (CH), 139.7 (Cq), 138.9 (Cq), 134.8 (Cq), 131.4 (CH), 131.3 (CH), 128.2 (CH), 127.1 (Cq), 124.0 (CH), 122.5 (CH), 119.3 (Cq), 104.2 (CH), 33.6 (Cq) and 31.2 (CH).

HRMS (MALDI): for $C_{66}H_{62}N_4NaO_4S_4Zn_2$ M+Na$^+$ = 1257.2104 (calculated) / M+Na$^+$ = 1257.2040 (found)

EA: for $C_{66}H_{62}N_4O_4S_4Zn_2.H_2O.Cl_2$, calculated: %C 59.91, %H 4.88, %N 4.23 / found (average on two trials): %C 59.98, %H 4.83, %N 4.28

5-(*tert*-butyl)-2-hydroxy-3-(thiophen-2-yl)benzaldehyde (**17**)

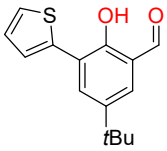

17

$C_{15}H_{16}O_2S$

M= 260.35 g.mol^{-1}

Under inert atmosphere, degassed 2-(tributylstannyl)thiophene (0.47 mL, 1.48 mmol, 3 equiv.) was added to a mixture of 5-(*tert*-butyl)-2-hydroxy-3-iodobenzaldehyde (0.150 g, 0.49 mmol, 1 equiv.), LiCl (209 mg, 4.93 mmol, 10 equiv.) and *trans*-dichlorobis(triphenylphosphine)palladium(II) (34 mg, 0.049 mmol, 10 mol%) in degassed dry DMF (3 mL). After heating to 100 °C for 24 h, the reaction mixture was concentrated then diluted with DCM (100 mL) and washed with aqueous ammonium chloride (3 × 30 mL). The organic layer was concentrated then filtered through silica, eluted with EtOAc and the solvent removed under vacuum to obtain a crude mixture, which was purified by silica gel chromatography (cyclohexane / ethyl acetate). The pure compound **17** was isolated as a bright yellow solid with a 50% yield.

Rf=0.8 (SiO_2, 90% cyclohexane + 10% ethyl acetate)

^{1}H NMR (500 MHz, CD_2Cl_2, 25 °C): δ = 11.74 (d, *J*=0.6 Hz, 1H), 9.94 (s, 1H), 7.94 (dd, *J*=2.4, 0.6 Hz, 1H), 7.63 (dd, *J*=3.7, 1.2 Hz, 1H), 7.54 (d, *J*=2.5 Hz, 1H), 7.39 (dd, *J*=5.2, 1.2 Hz, 1H), 7.14 (dd, *J*=5.2, 3.7 Hz, 1H) and 1.38 (s, 9H).

^{13}C NMR (126 MHz, CD_2Cl_2, 25 °C): δ = 197.8 (CH), 156.1 (Cq), 143.3 (Cq), 138.4 (Cq), 133.6 (CH), 130.0 (CH), 127.6 (CH), 126.6 (CH), 126.1 (CH), 123.0 (Cq), 121.0 (Cq), 34.5 (Cq) and 31.4 (CH_3).

HRMS (DCI): for $C_{15}H_{17}O_2S$ MH^+ = 261.0949 (calculated) / MH^+ = 261.0956 (found)

Bis-salophen Zn(II) complex **18**

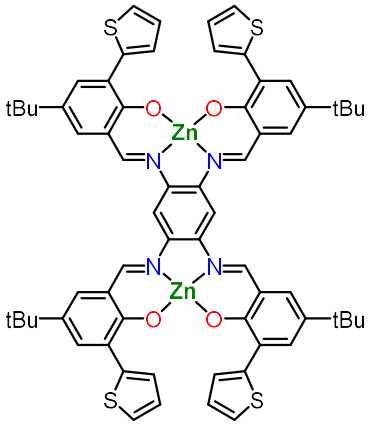

18

$C_{66}H_{62}N_4O_4S_4Zn_2$

M= 1234.25 g.mol^{-1}

Under inert atmosphere, 1,2,4,5-benzenetetramine tetrahydrochloride (0.053 mmol, 15 mg, 1 equiv.) and zinc diacetate dihydrate (0.21 mmol, 46 mg, 4 equiv.) were dispersed in DMSO (2.25 mL) to afford a dark red solution. After stirring for a few minutes, the 5-(*tert*-butyl)-2-hydroxy-3-(thiophen-2-yl)benzaldehyde **17** (0.21 mmol, 55 mg, 4 equiv.) was dissolved in 0.75 mL of DMSO and added to the dark red solution. The mixture was stirred at 60 °C for 48 h. Upon completion of the reaction (TLC monitoring), water was added (20 mL) in order to precipitate the product, which was collected by filtration and washed respectively with methanol and acetonitrile. After drying in vacuo, complex **18** was obtained as a brick red solid with a 85% yield.

^{1}H NMR (300 MHz, DMSO-d$_6$, 25 °C): δ = 9.27 (s, 4H), 8.41 (s, 2H), 7.99 (d, *J*=3.7 Hz, 4H), 7.94 (d, *J*=2.6 Hz, 4H), 7.51 (d, *J*=2.6 Hz, 4H), 7.47 (d, *J*=5.2 Hz, 4H), 7.13 (t, *J*=4.4 Hz, 4H) and 1.39 (s, 36H).

^{13}C NMR (126 MHz, DMSO-d$_6$, 25 °C): δ = 166.2 (Cq), 163.6 (CH), 140.6 (Cq), 139.1 (Cq), 134.9 (Cq), 131.5 (CH), 129.2 (CH), 126.2 (CH), 125.6 (Cq), 124.7 (CH), 123.4 (CH), 119.4 (Cq), 104.6 (CH), 33.6 (Cq) and 31.4 (CH_3).

HRMS (ESI): for $C_{66}H_{62}N_4O_4S_4Zn_2$ M^{2+} = 618.1182 (calculated) / M^{2+} = 618.1201 (found)

EA: for $C_{66}H_{62}N_4O_4S_4Zn_2.2H_2O$, calculated: %C 62.41, %H 5.24, %N 4.41 / found (average on two trials): %C 62.56, %H 4.865, %N 4.325

II. Synthesis and characterization of hybrid materials

Platinum nanoparticles

The Pt nanoparticles have been synthesized as followed. [8, 9] All operations were carried out using Fischer-Porter bottle techniques under argon. A solution of $Pt_2(dba)_3$ (90 mg; 0.165 mmol of Pt) in 20 mL of freshly distilled and deoxygenated THF was pressurized in a Fischer-Porter bottle with 1 bar of CO during 30 minutes at room temperature under vigorous stirring. During this time, the solution color changed from violet to brown (attesting the formation of the nanoparticles). The mixture was evaporated and washed with pentane to eliminate the dba (3 x 20 mL), and to obtain native nanoparticles. The colloid was then redissolved in 20 mL of THF.

Self-assembly

1 mL of a solution of bis-salophen (at 6.10^{-3} mol.L^{-1} in THF) was added to 4 mL of the native nanoparticle mixture under vigorous mixing. The precursor concentrations were adapted to obtain 0.05 equivalent number of bis-salophen per introduced Pt. The brown solution was agitated for 2 hours. Drops of the crude solution were deposited on specific substrates for each characterization (see below). The remaining solution was evaporated to dryness and was isolated as dark-brown powder.

Structural characterization of nanoparticles and self-assemblies

Transmission Electron Microscopy.

Samples for TEM were prepared by deposition of one drop of the crude solution on a carbon covered holey copper grid. TEM analyses were performed at the "centre de microcaractérisation Raimond Castaing" using a JEOL JEM 1400 electron microscope operating at 120 kV. The mean size of the particles was determined by image analysis on a large number of particles (~300) using the ImageJ software. The size of the nanoparticles was found to be 1.4 ± 0.3 nm.

Infrared spectroscopy.

FT-IR spectra were recorded on a Thermo Scientific Nicolet 6700 FT-IR spectrometer in the range 4000-700 cm^{-1}, using a Smart Orbit ATR platform. The sample deposition was performed by drop casting of the crude solution on the germanium crystal of the platform; the measurement was acquired after evaporation of the THF solvent.

Small angle X-ray scattering.

SAXS patterns were recorded on a PANalytical Empyrean diffractometer using the Co Kα radiation. Small angle measurements were performed on a microscopy glass, on which the crude solution was drop casted. An advantage of working with particles smaller than 2 nm is that the inter-particle distance is sufficiently small to observe correlation distances between two particles with a regular XRD diffractometer without the need of any dedicated SAXS facilities.

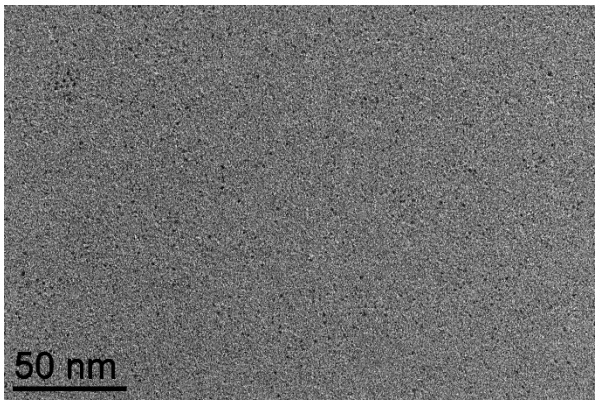

Figure S1. TEM picture of the naked nanoparticles.

(a)

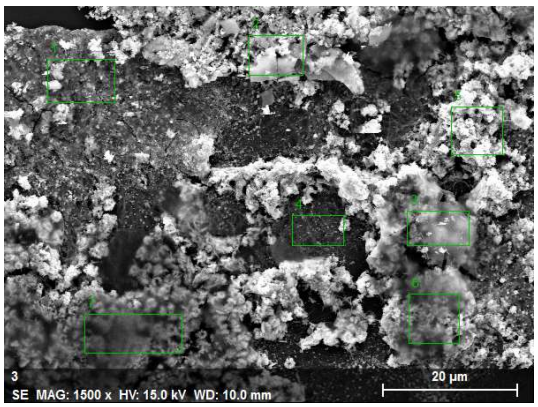

(b)

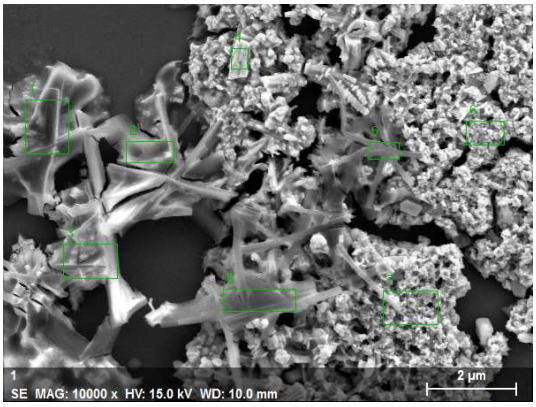

Figure S2. SEM pictures of (a) **SA-16** and (b) **SA-18**. Zn:Pt elemental ratios obtained by probing zones represented by squares on the pictures : **SA-16** : Zn:Pt = 0.08 thus bis-salophen:Pt = 0.04 ; **SA-18** : Zn:Pt = 0.14 thus bis-salophen:Pt = 0.07. Bis-salophen:Pt ratios are in good agreement with the theoretical value of 0.05 for the introduced components.

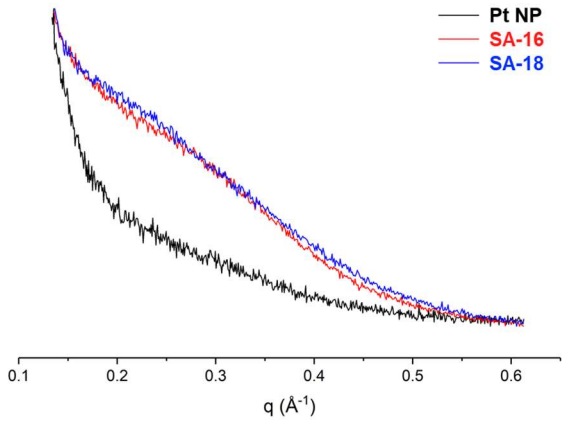

Figure S3: Small angle X-Ray scattering (SAXS) for Pt NP, and for the **SA-16**, and **SA-18** self-assemblies. The reference Pt NP does not show any specific pattern, whereas the self-assemblies show a supplementary broad peak at q = 0.28 $Å^{-1}$, which corresponds to a specific correlation distance between the nanoparticles. The associated inter-nanoparticle correlation distance (s = 2π / qmax) was estimated to 2.3 nm for both **SA-16** and **SA-18**

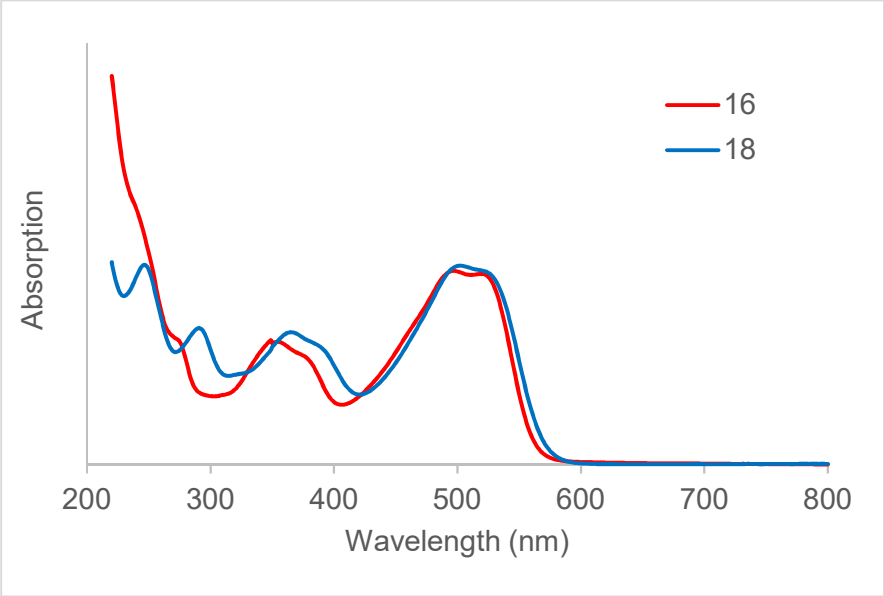

Figure S4. UV-vis spectra of the complexes **16** and **18**.

Charge transport measurements

I-V curve measurements.

Conductive AFM measurements were performed with an AIST-NT SmartSPM 1000 microscope, equipped with a conductive AFM unit. The samples were prepared by drop casting of one drop of the crude solution on silicon wafers covered by a ~50 nm layer of gold (with a ~5 nm chromium anchoring layer). We used conductive silicon tips covered by platinum (Mikromash HQ-NSC15/Pt). Typical measurements consisted in first performing a topography image of the sample and then going in contact on zones with individual assemblies to measure their *I-V* characteristics. Measurements were performed on several objects per zone and several zones of the substrates. Our system allows current measurements between 10 pA and 100 nA, the amplitude of the current decreasing with the size of the objects.

Data analysis.

The *I-V* characteristics were normalized at 2 V. We then averaged the characteristics on 50 curves (error bars on the graphs are 95% confidence intervals).

Measurements under light irradiation.

For measurements under light irradiation, a green laser at 532 nm was focalized at the interface between the AFM tip and the substrate, thanks to a HORIBA coupled system, initially conceived for Raman cartography. The laser power was measured at 10 mW at the location of the surface. The variation of current was measured at a voltage of 2 V whereas light was successively switched on and

off every 10 s. The variation of current was calculated as the ratio between the current value before and after the light switching, and averaged on 60 on-off switches to estimate the response of the different samples.

III. NMR spectra of synthetic intermediates and targets

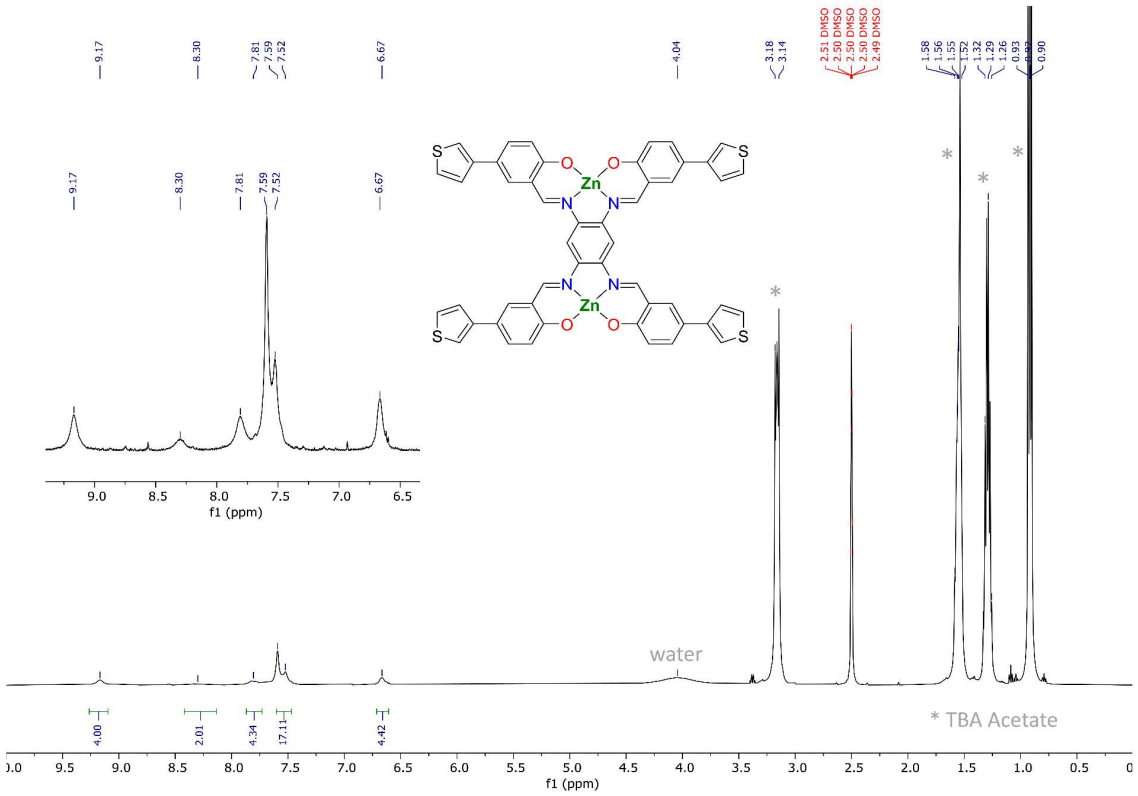

Figure S5: ^{1}H NMR spectrum (500 MHz) of **3** in DMSO-d_6 (+ TBA Acetate)

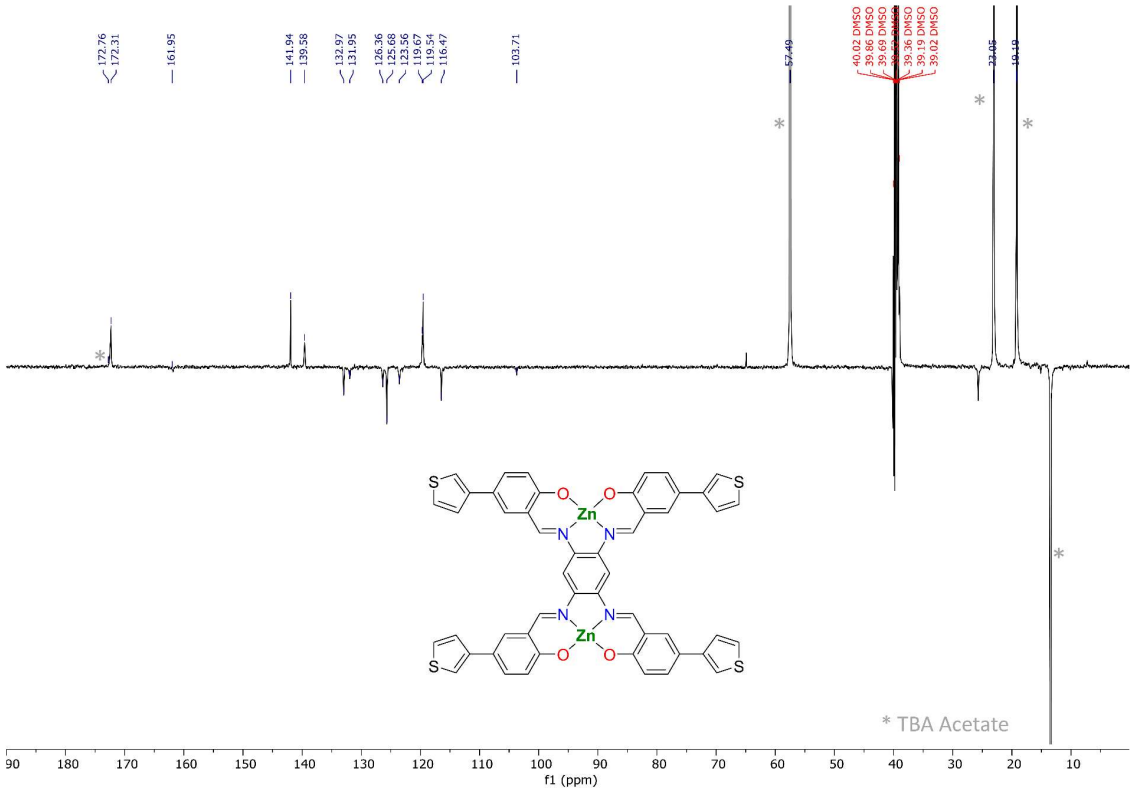

Figure S6: ^{13}C NMR spectrum (126 MHz) of **3** in DMSO-d_6 (+ TBA Acetate)

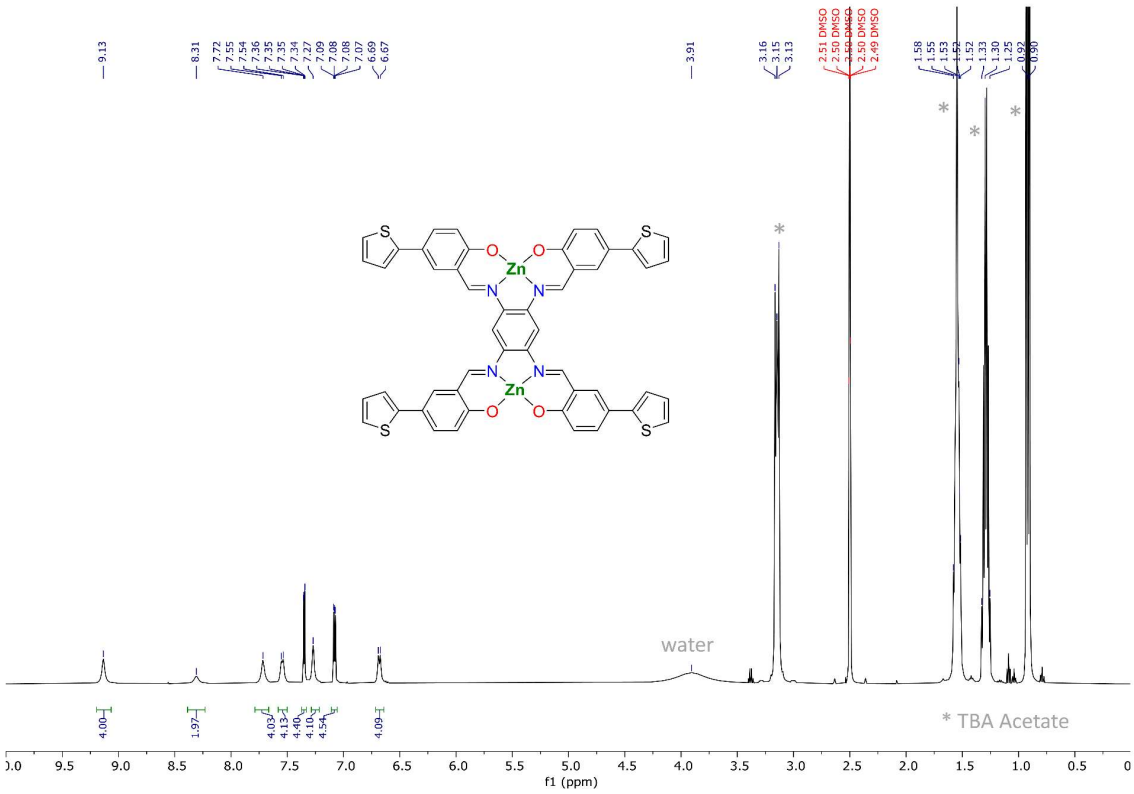

Figure S7: ^{1}H NMR spectrum (500 MHz) of **5** in DMSO-d_6 (+ TBA Acetate)

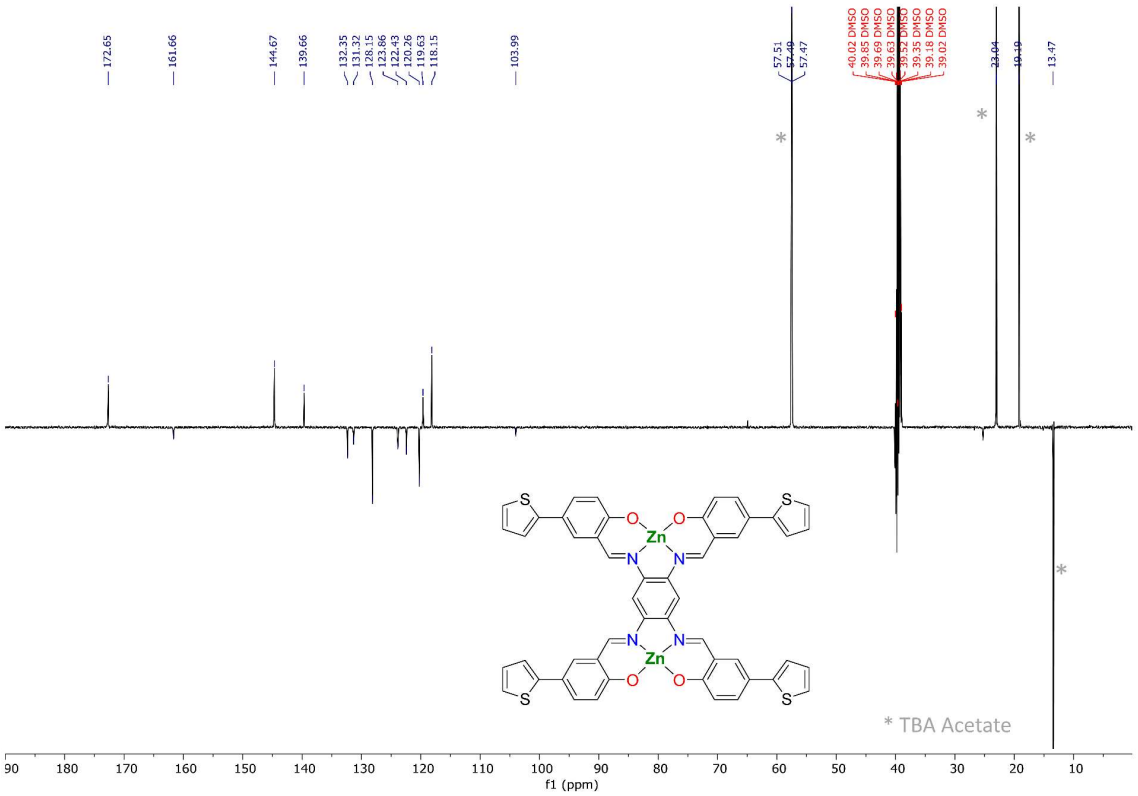

Figure S8: ^{13}C NMR spectrum (126 MHz) of **5** in DMSO-d_6 (+ TBA Acetate)

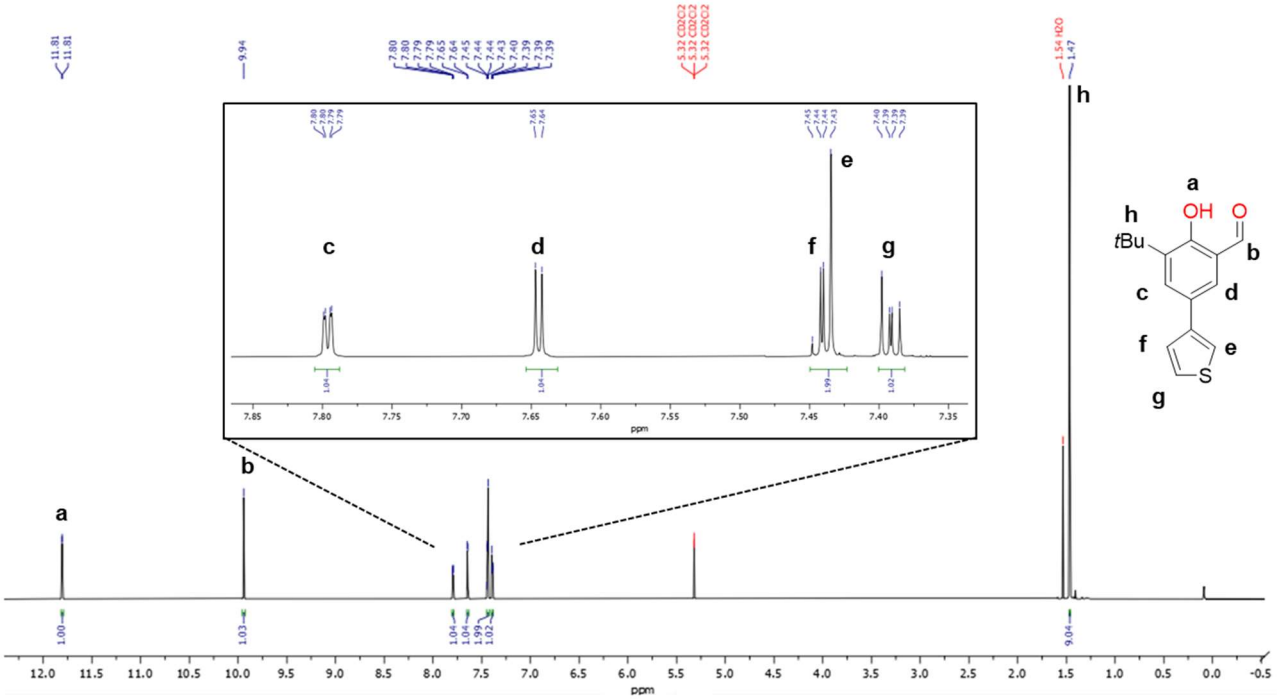

Figure S9: ^{1}H NMR spectrum (500 MHz) of **7** in CD_2Cl_2

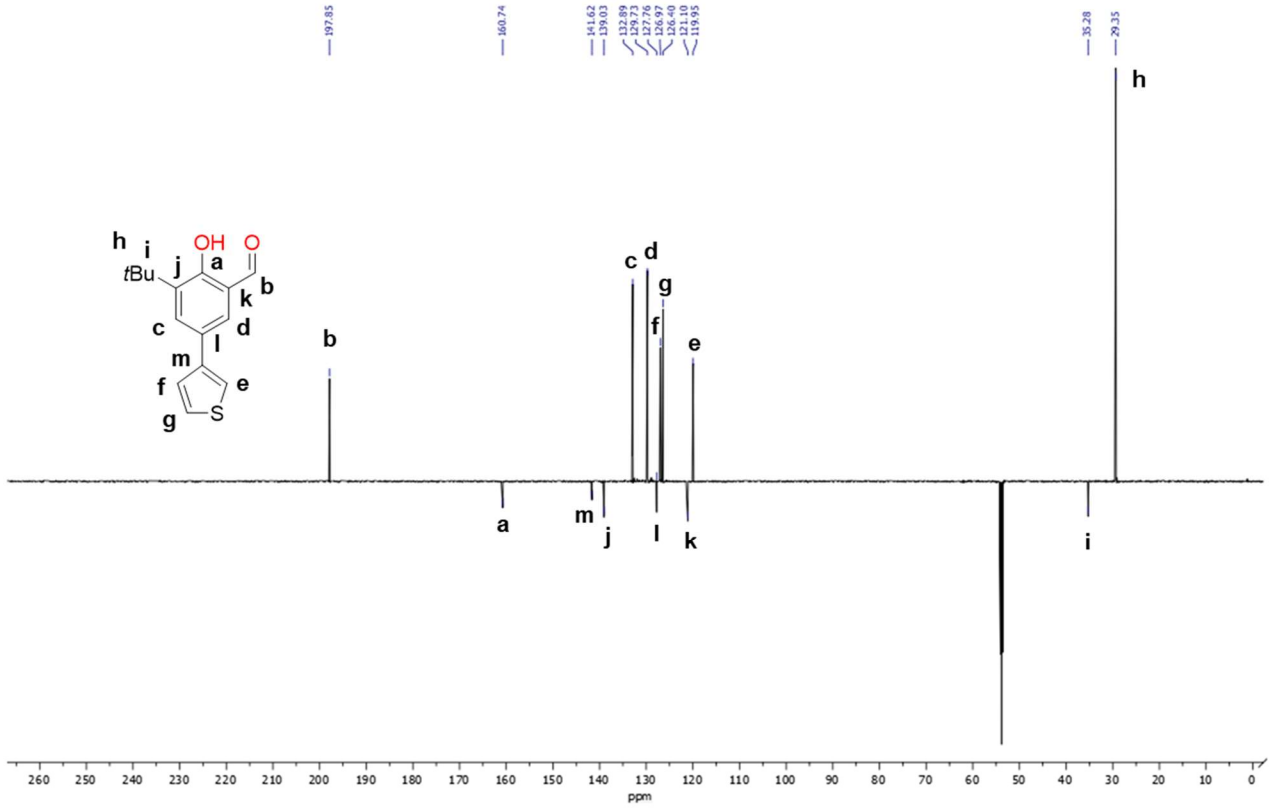

Figure S10: ^{13}C NMR spectrum (126 MHz) of **7** in CD_2Cl_2

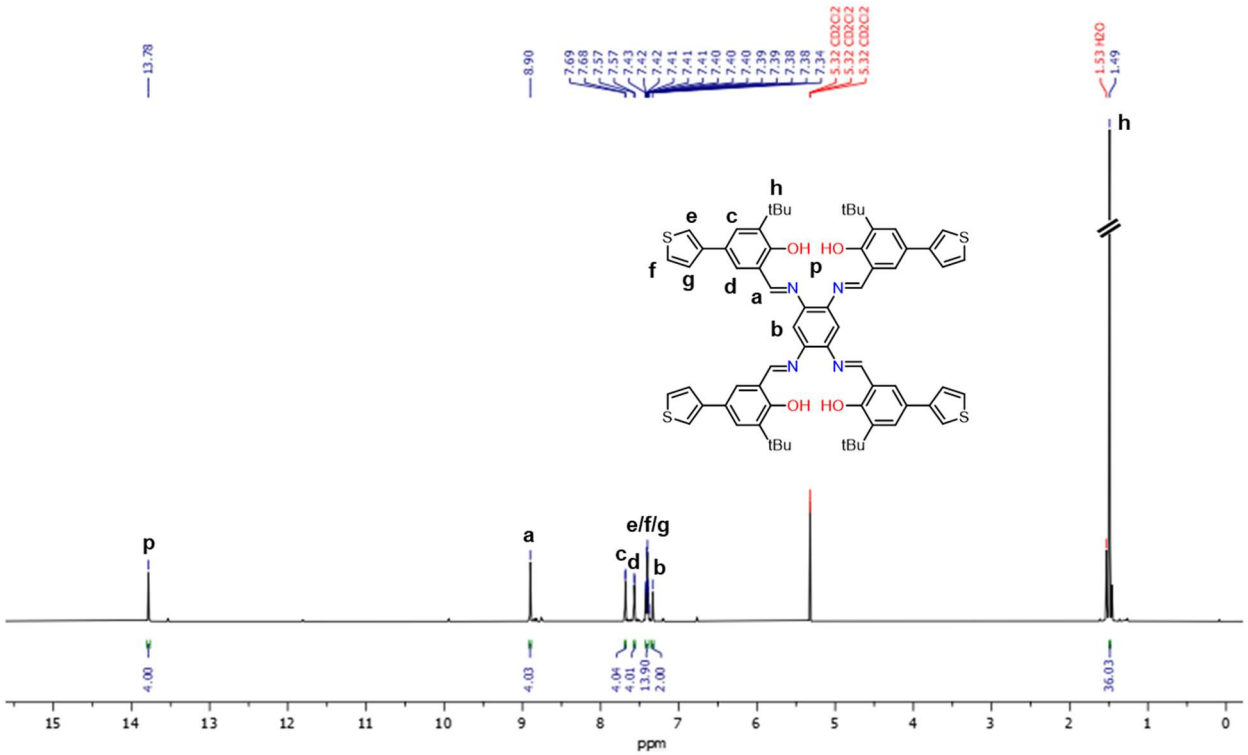

Figure S11: ^{1}H NMR spectrum (500 MHz) of **8** in CD_2Cl_2 and proposed attribution of resonances

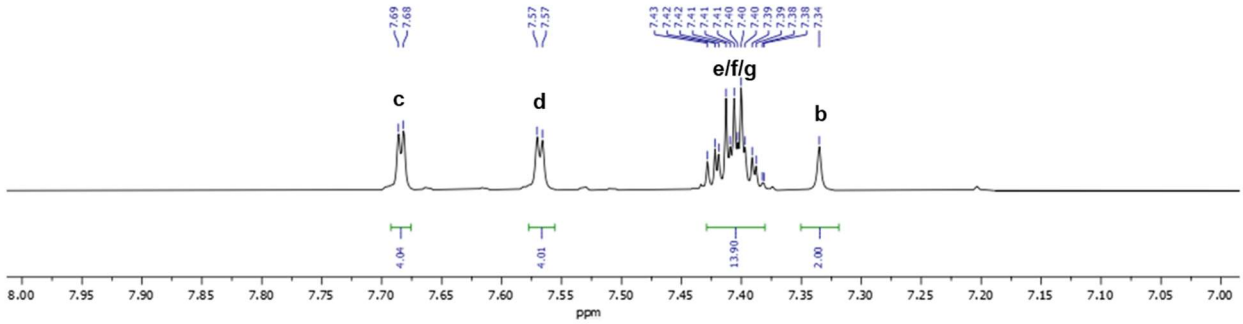

Figure S12: ^{1}H NMR spectrum (500 MHz) of **8** in CD_2Cl_2 (zoom in the 8.00 – 7.00 ppm region)

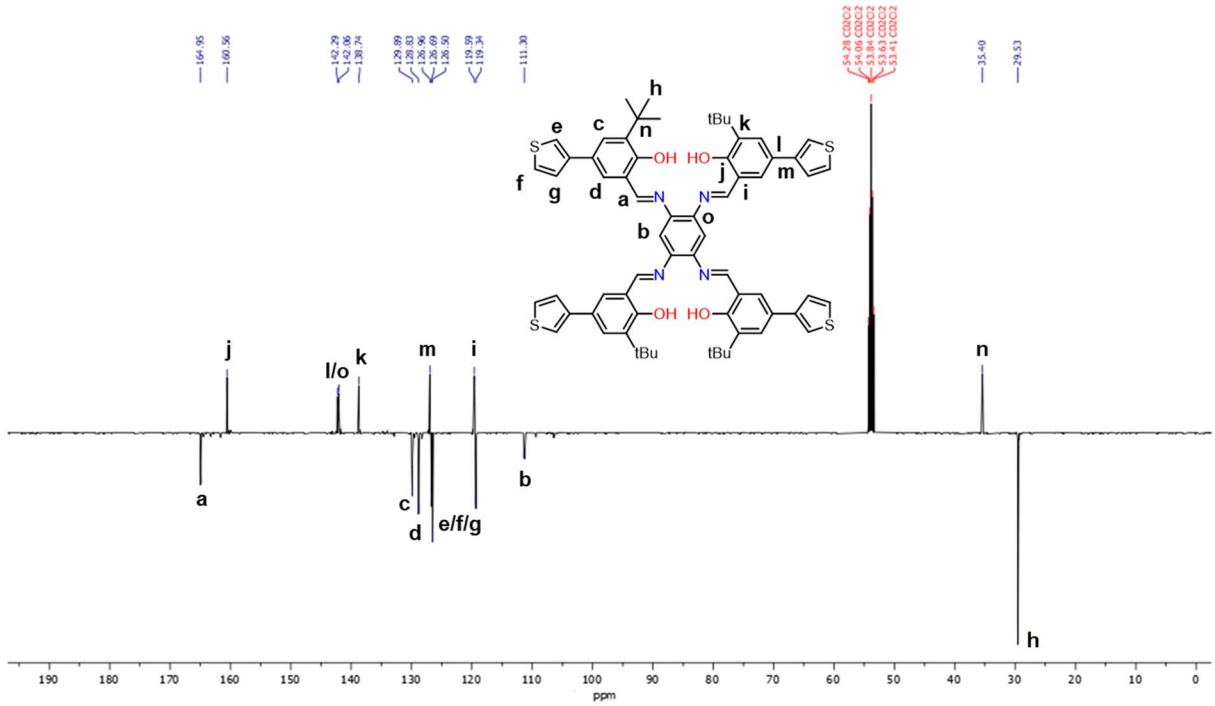

Figure S13: ^{13}C NMR spectrum (126 MHz) of **8** in CD_2Cl_2 and proposed attribution of resonances (traces of impurities on the baseline – compound was used as such in next step)

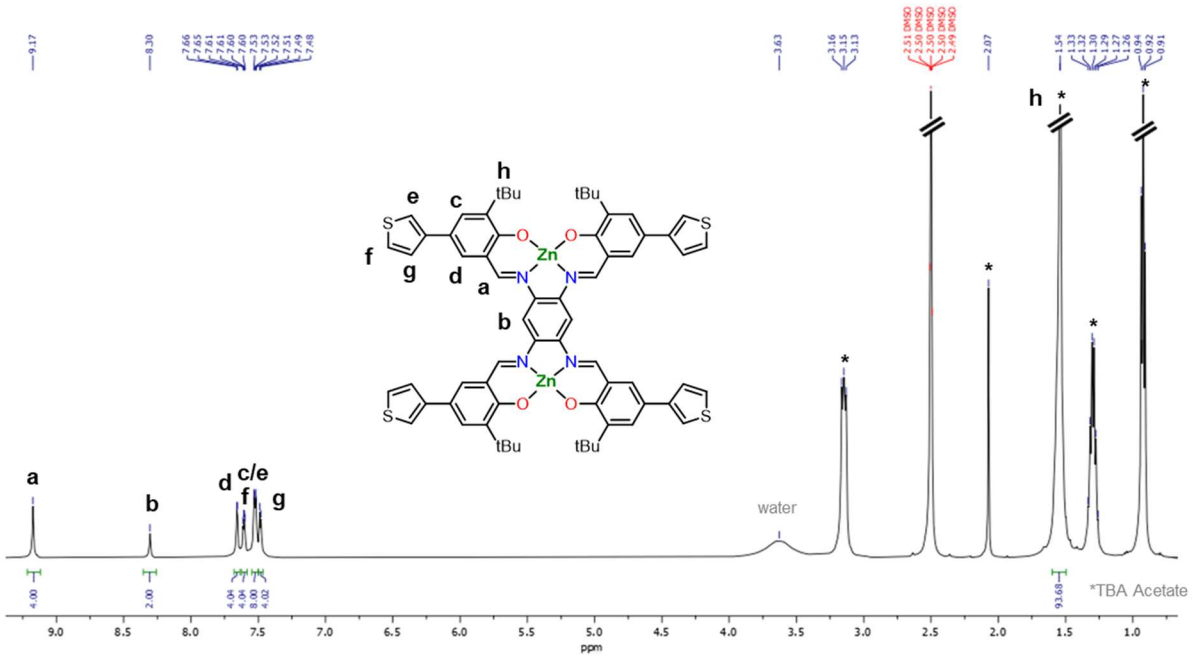

Figure S14: ^{1}H NMR spectrum (500 MHz) of **9** in DMSO-d_6 (+ TBA Acetate) and proposed attribution of resonances (traces of acetonitrile and presence of TBA Acetate)

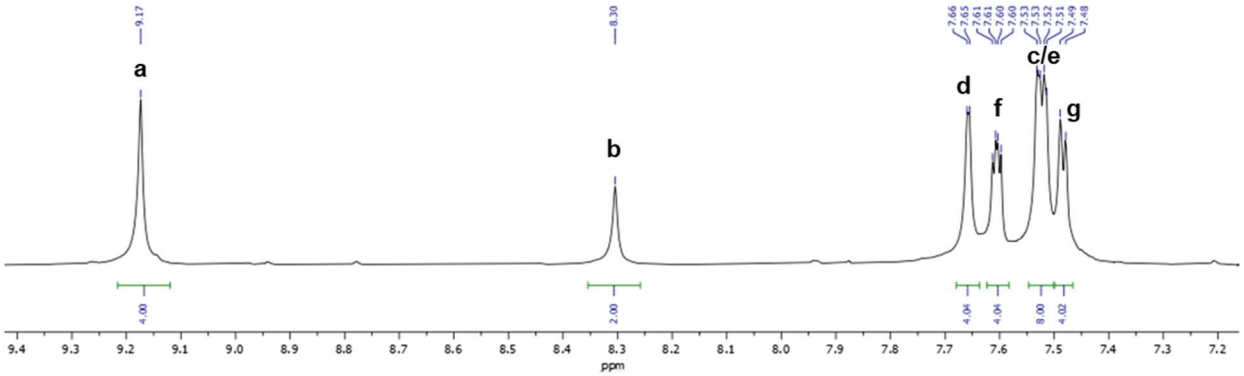

Figure S15: ^{1}H NMR spectrum (500 MHz) of **9** in DMSO-d_6 (+ TBA Acetate) (zoom in the 9.40 – 7.20 ppm region)

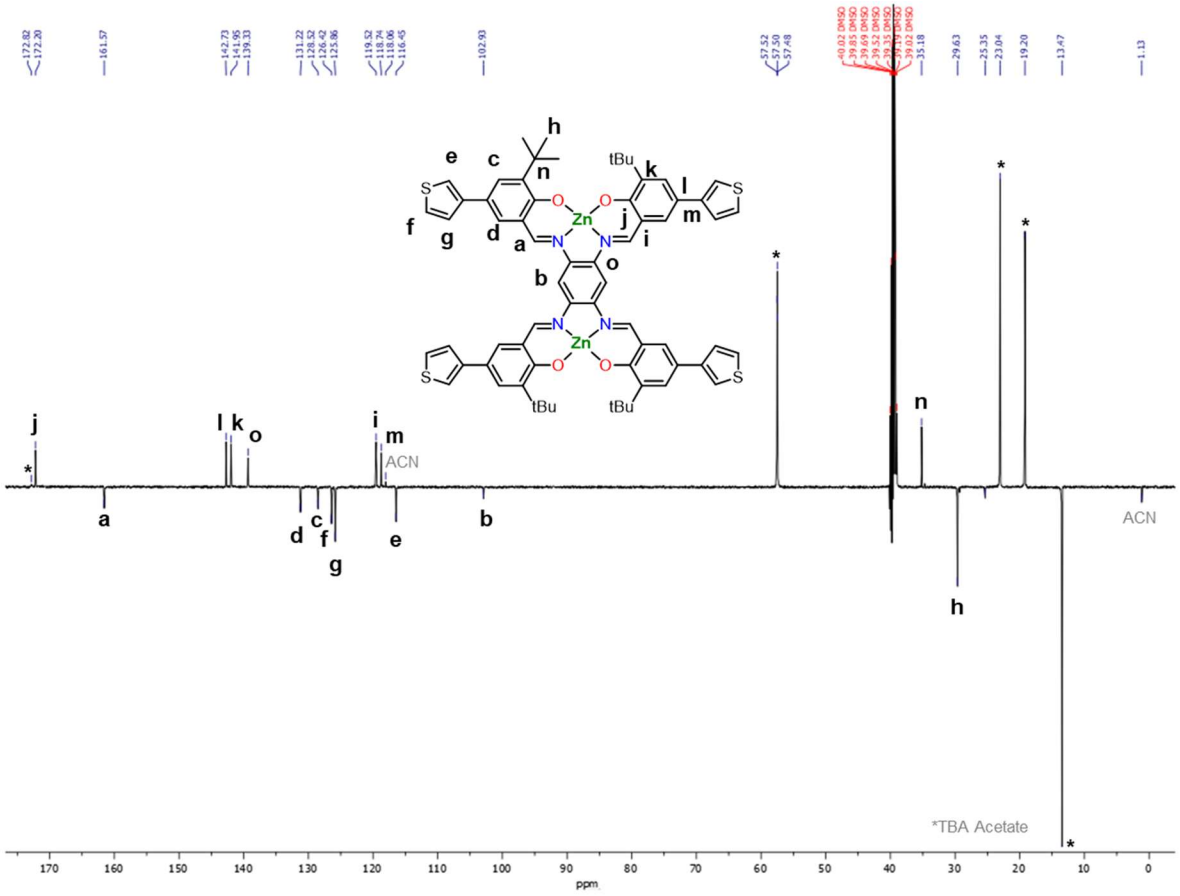

Figure S16: ^{13}C NMR spectrum (126 MHz) of **9** in DMSO-d_6 (+ TBA Acetate) and proposed attribution of resonances (traces of acetonitrile and presence of TBA Acetate)

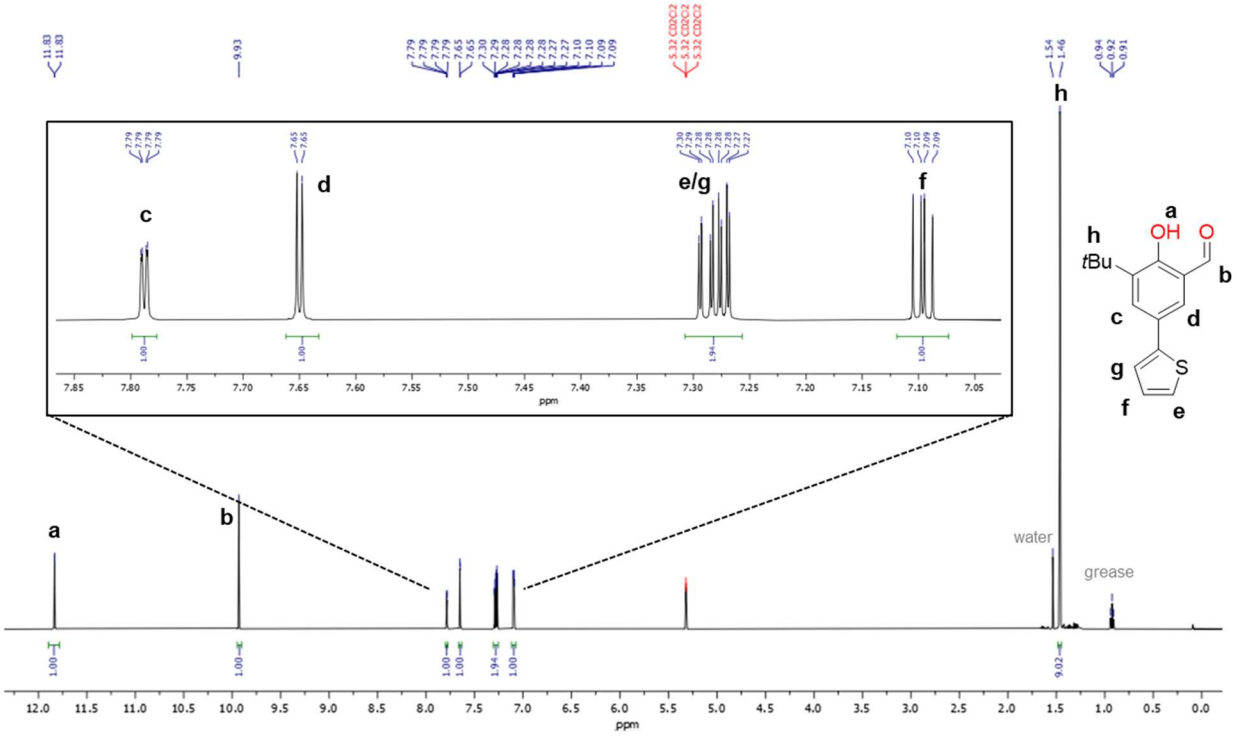

Figure S17: ^{1}H NMR spectrum (500 MHz) of **11** in CD_2Cl_2 (and zoom in the 7.85 – 7.05ppm region)

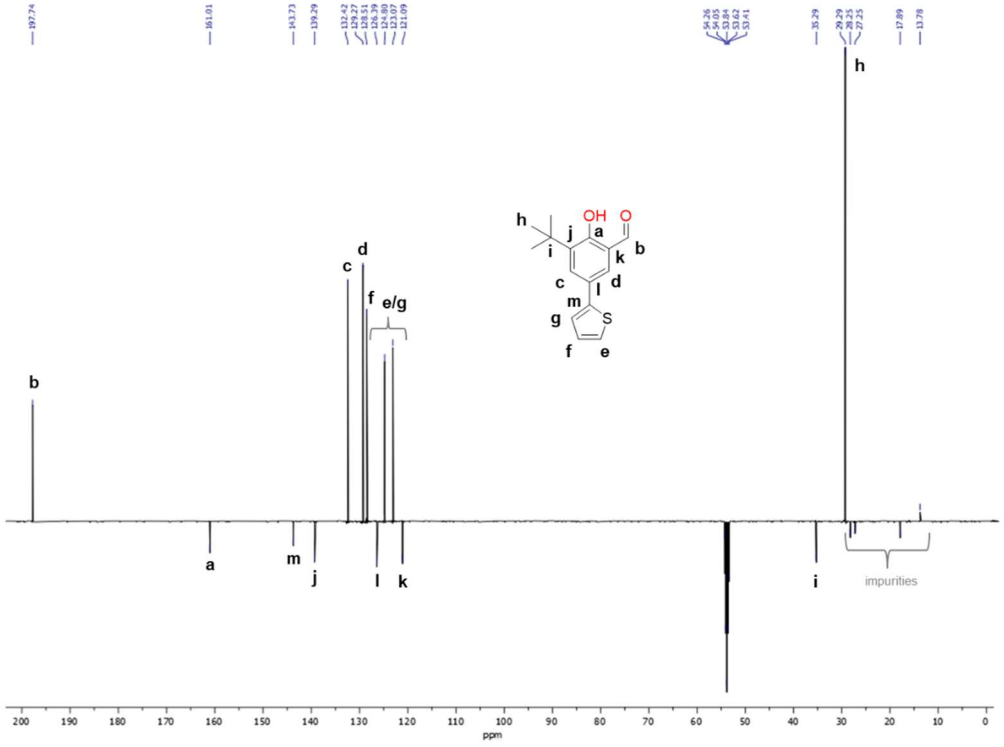

Figure S18: ^{13}C NMR spectrum (126 MHz) of **11** in CD_2Cl_2 and proposed attribution of resonances

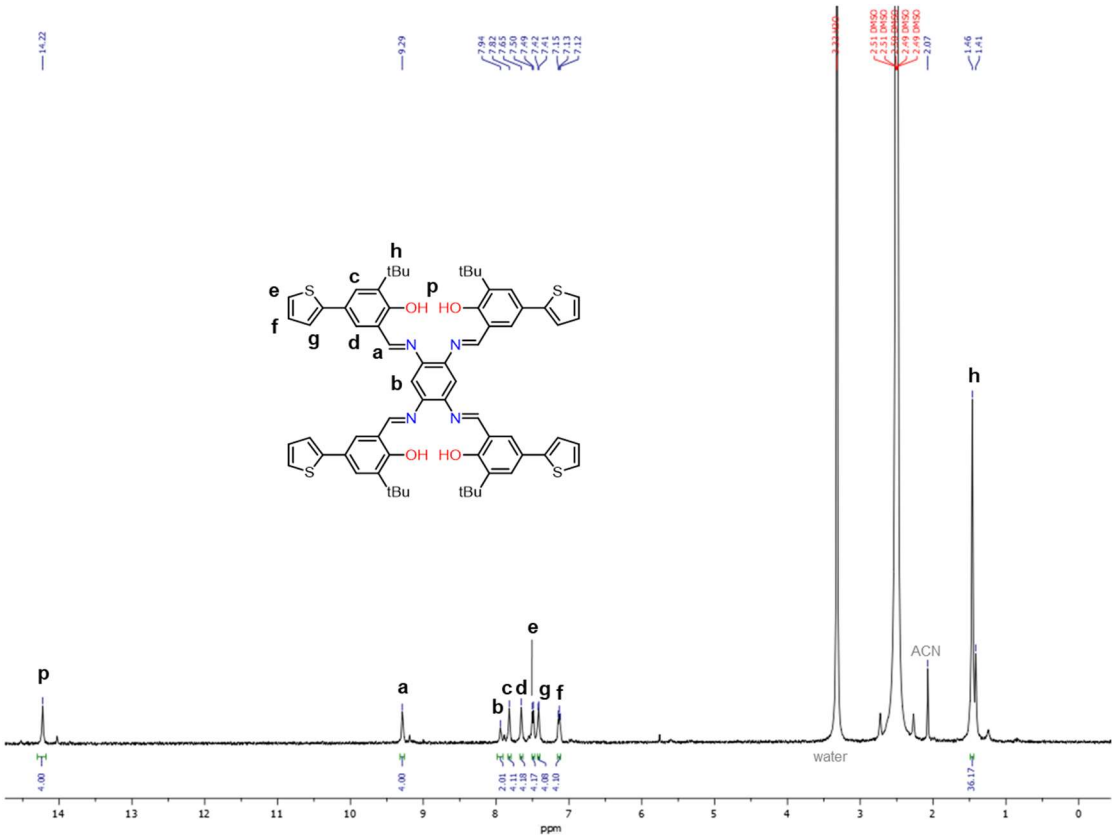

Figure S19: ^{1}H NMR spectrum (300 MHz) of **12** in DMSO-d_6

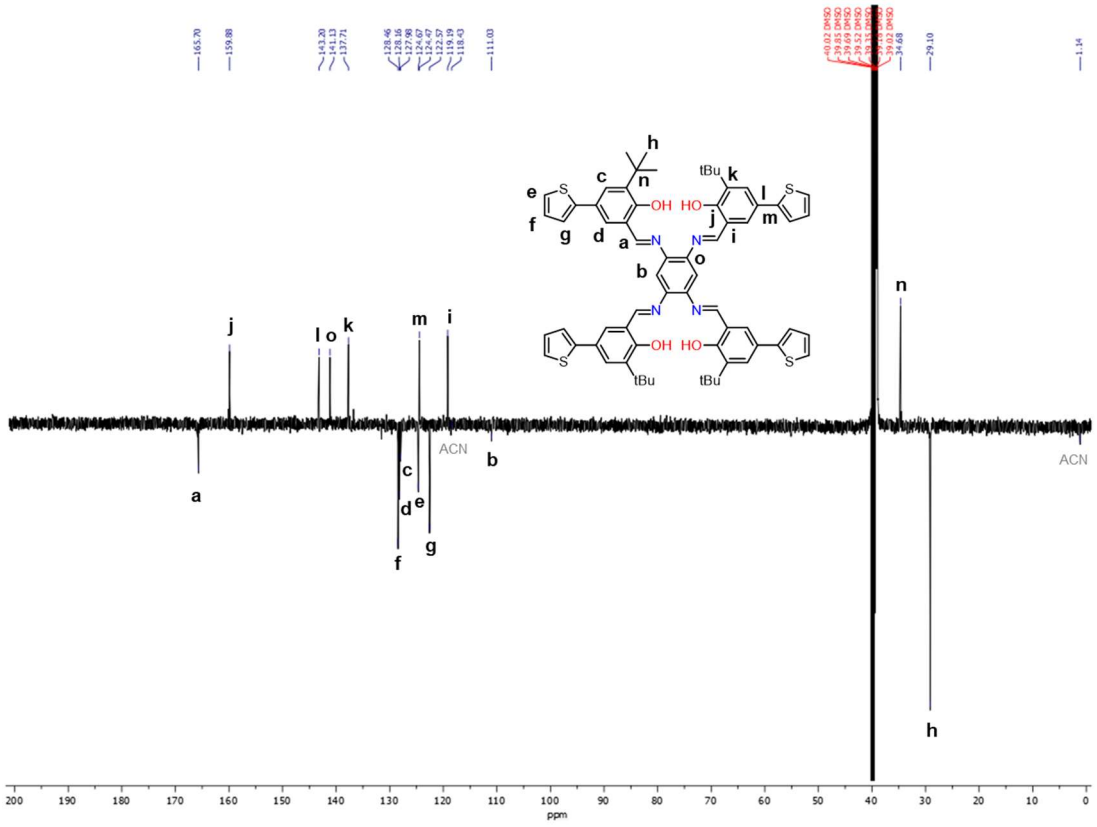

Figure S20: ^{13}C NMR spectrum (126 MHz) of **12** in DMSO-d_6 and proposed attribution of resonances

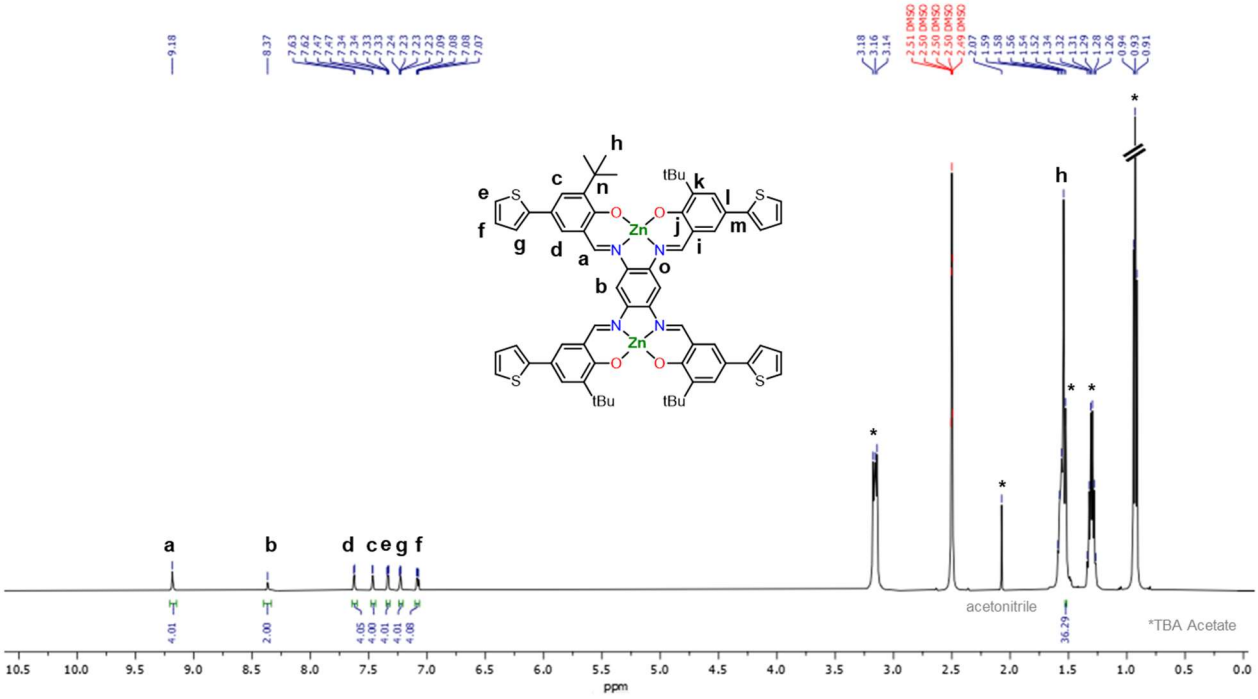

Figure S21: ^{1}H NMR spectrum (500 MHz) of **13** in DMSO-d_6 (+ TBA Acetate) and proposed attribution of resonances (traces of acetonitrile and presence of TBA Acetate)

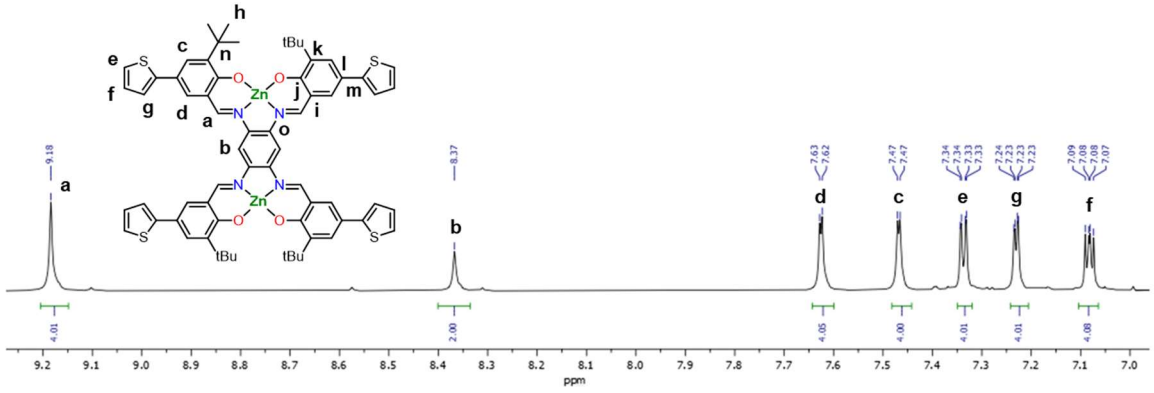

Figure S22: ^{1}H NMR spectrum (500 MHz) of **13** in DMSO-d_6 (+ TBA Acetate) (zoom in the 9.20 – 7.00 ppm region)

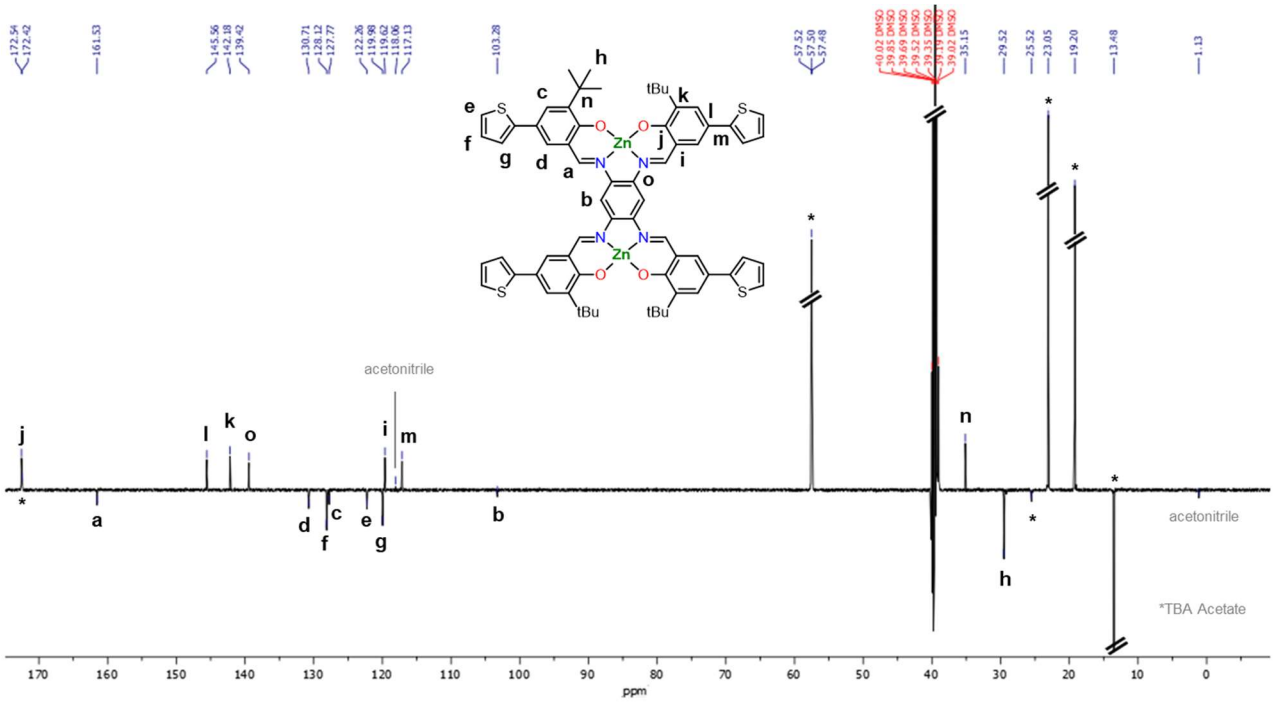

Figure S23: ^{13}C NMR spectrum (126 MHz) of **13** in DMSO-d_6 (+ TBA Acetate) and proposed attribution of resonances (traces of acetonitrile and presence of TBA Acetate)

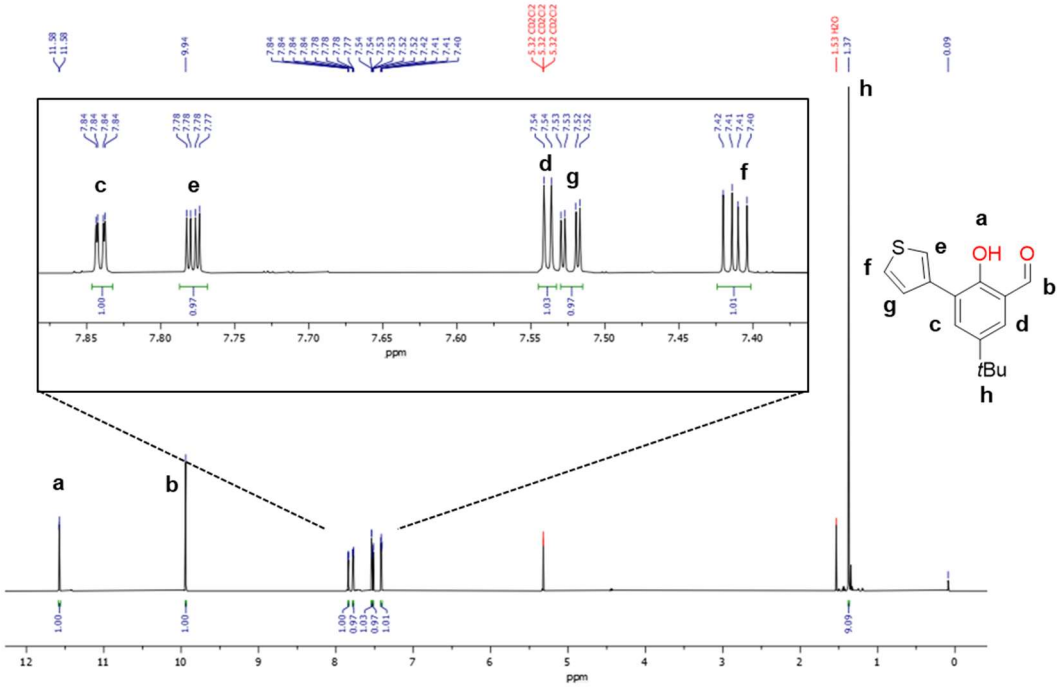

Figure S24: ^{1}H NMR spectrum (500 MHz) of **15** in CD_2Cl_2 (and zoom in the 7.85 – 7.40 ppm region), presence of water at 1.53 ppm and silicon grease at 0.09ppm and proposed attribution of resonances.

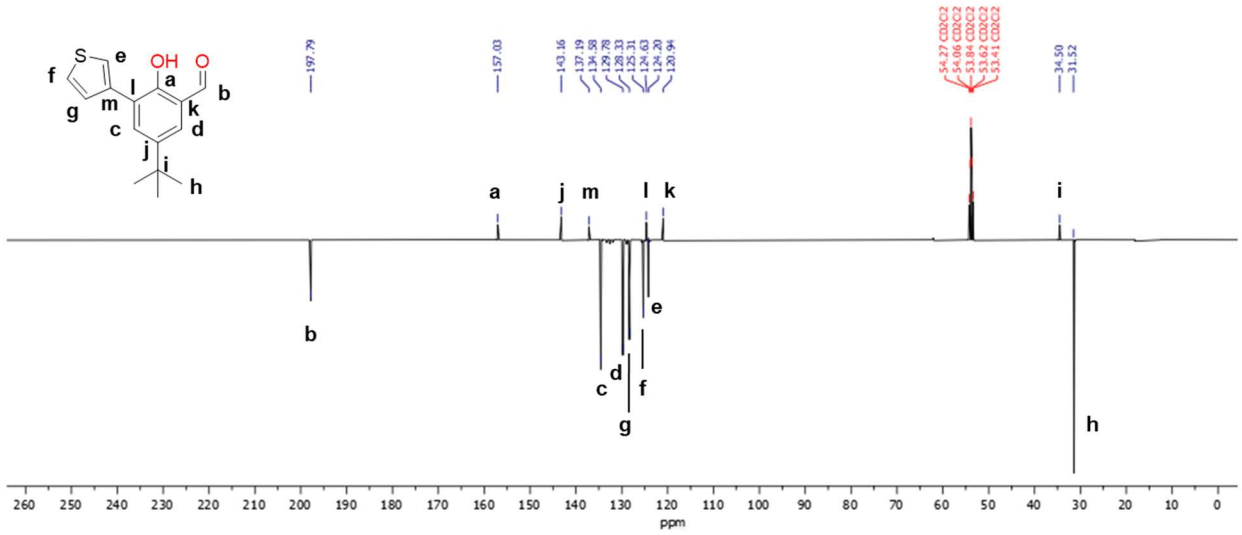

Figure S25: ^{13}C NMR spectrum (126 MHz) of **15** in CD_2Cl_2 and proposed attribution of resonances

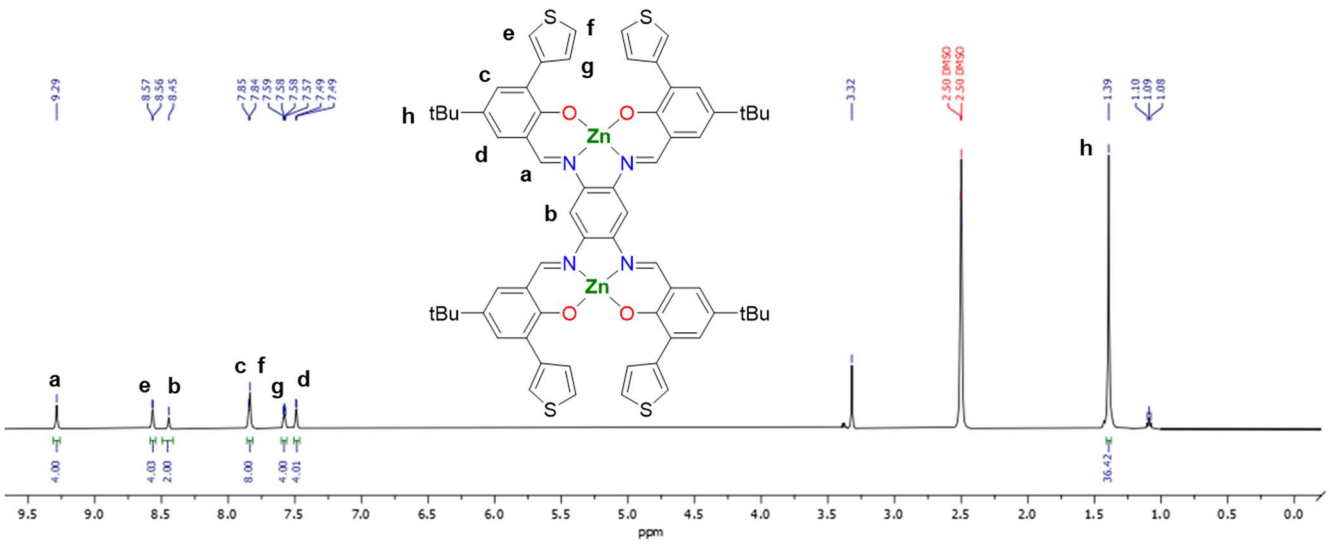

Figure S26: ^{1}H NMR spectrum (500 MHz) of **16** in DMSO-d_6 (Presence of residual Et_2O: quadruplet at 3.38 ppm and triplet at 1.09 ppm)

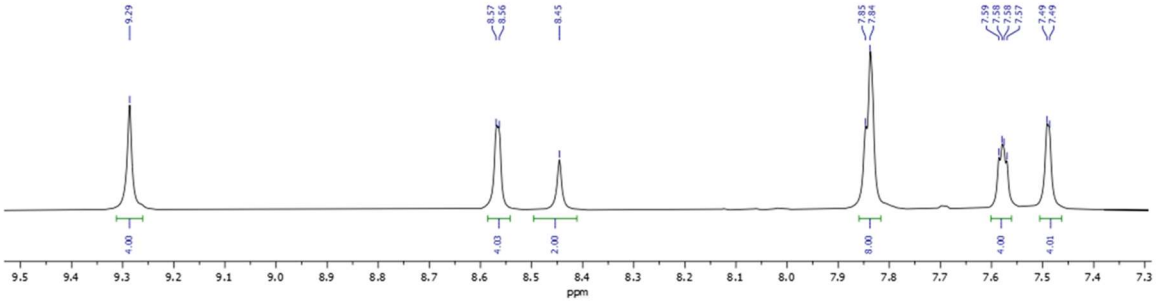

Figure S27: ^{1}H NMR spectrum (500 MHz) of **16** in DMSO-d_6 (zoom in the 9.50 – 7.30ppm region)

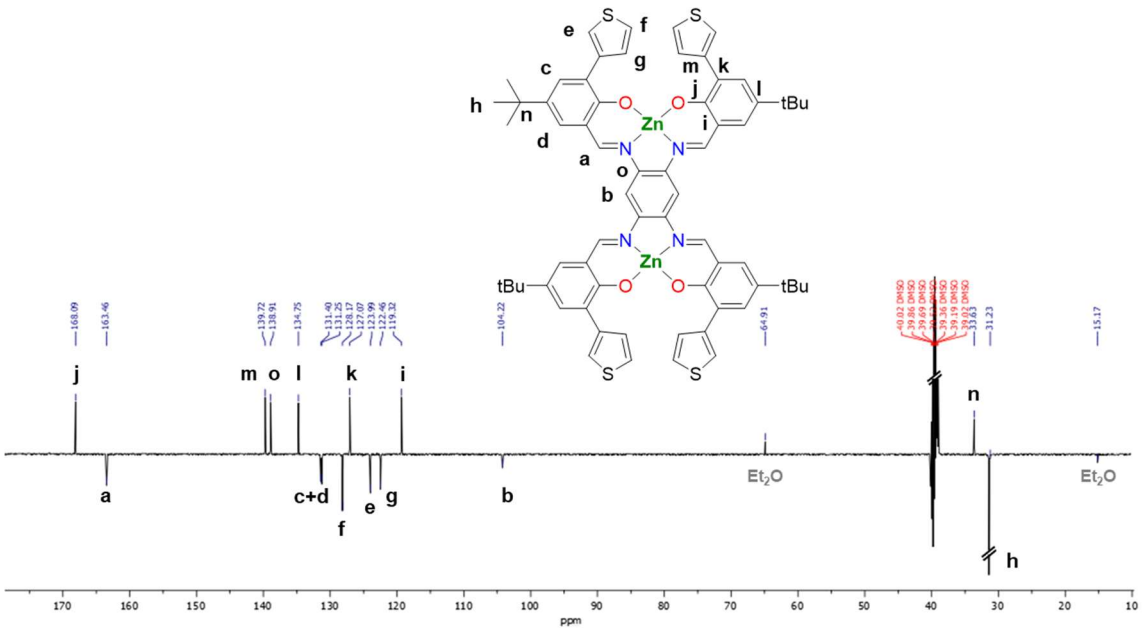

Figure S28: ^{13}C NMR spectrum (126 MHz) of **16** in DMSO-d_6 and proposed attribution of resonances

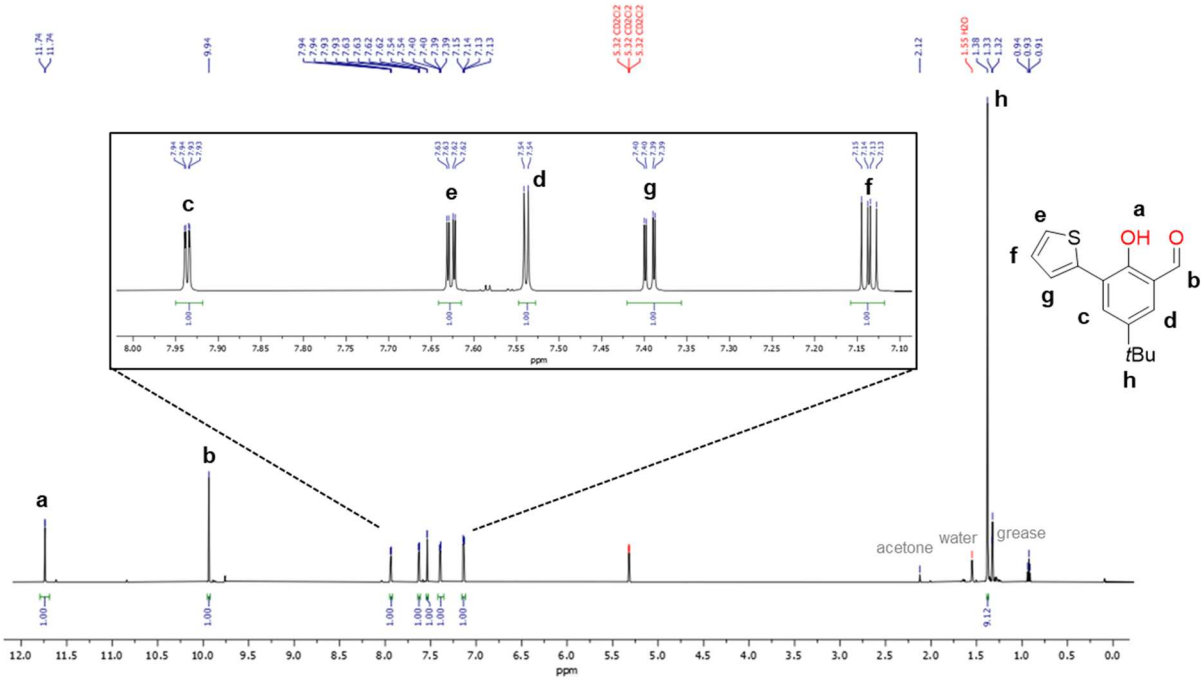

Figure S29: ^{1}H NMR spectrum (500 MHz) of **17** in CD_2Cl_2 (with zoom in the 8.00 – 7.00ppm region)

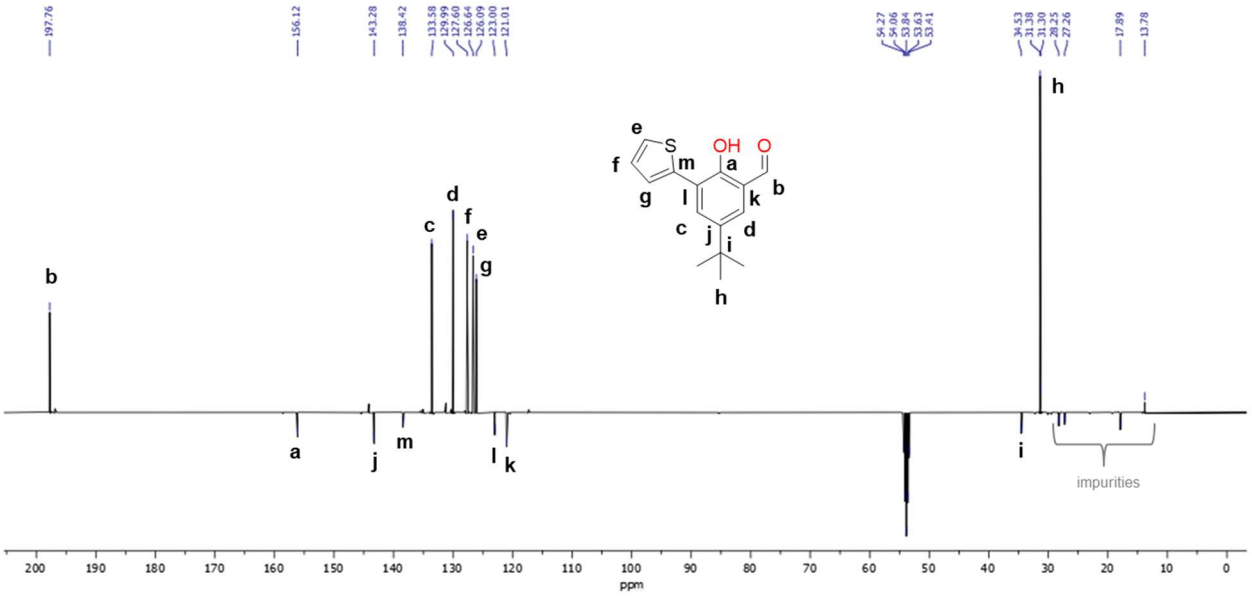

Figure S30: ^{13}C NMR spectrum (126 MHz) of **17** in CD_2Cl_2 and proposed attribution of resonances

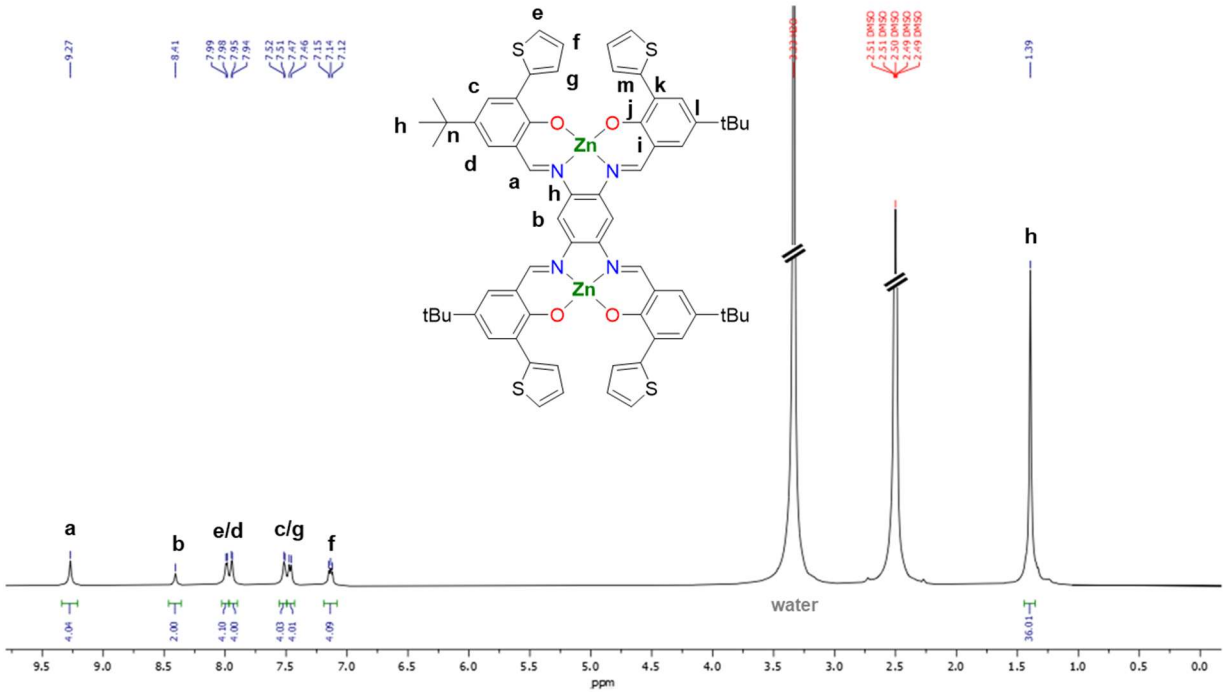

Figure S31: ^{1}H NMR spectrum (300 MHz) of **18** in DMSO-d_6

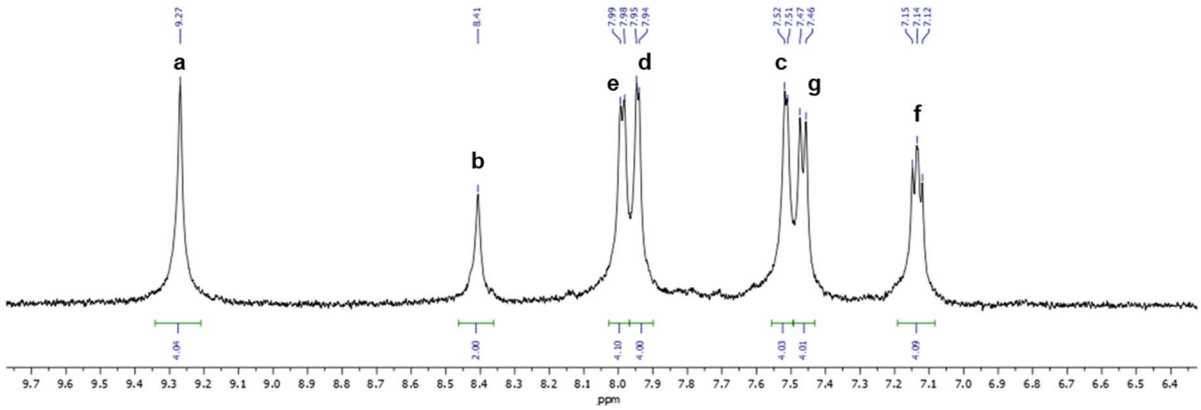

Figure S32: ^{1}H NMR spectrum (300 MHz) of **18** in DMSO-d_6 (zoom in the 9.70 – 6.40ppm region)

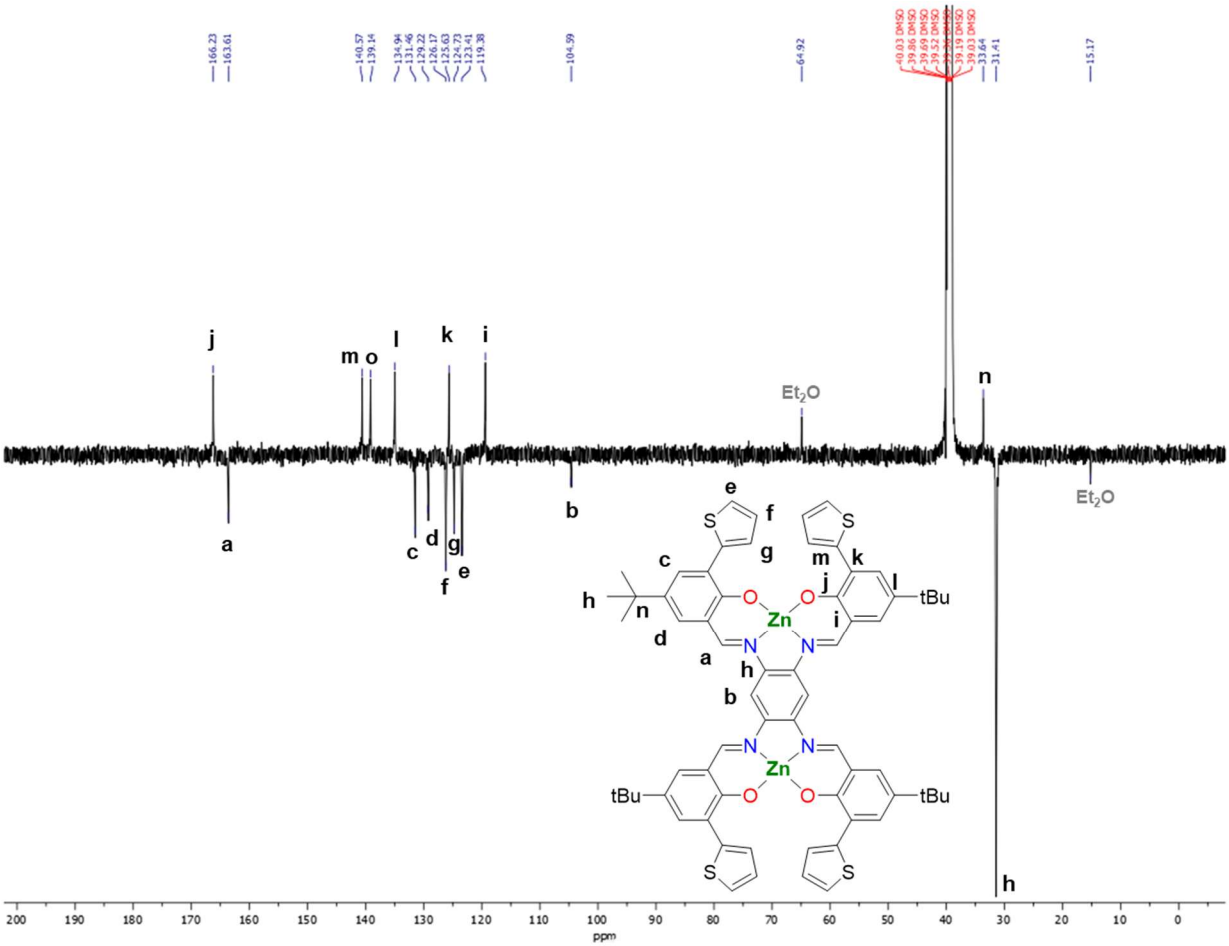

Figure S33: ^{13}C NMR spectrum (126 MHz) of **18** in DMSO-d_6 and proposed attribution of resonances

IV. Crystallographic data of molecular targets

Table S1: Crystallographic parameters for tetra–Schiff bases **8**, **12** and complexes **13**, **16**, **18**

Compound	**8**	**12**	**13**	**16**	**18**
Empirical formula	C66 H66 N4 O4 S4, 2 (CH2 Cl2)	C66 H66 N4 O4 S4, 3 (CH2 Cl2)	C72 H74 N4 O6 S4 Zn2, 2 (C3 H6 O)	C70 H74 N4 O6 S6 Zn2, 6 (C2 H6 O S)	C70 H74 N4 O6 S6 Zn2, 6 (C2 H6 O S)
M (g mol–1)	1277.32	1362.24	1466.48	1859.19	1859.19
Crystal size (mm^3)	0.400 x 0.080 x 0.040	0.400 x 0.050 x 0.030	0.080 x 0.030 x 0.020	0.150 x 0.060 x 0.050	0.200 x 0.060 x 0.040
Space group	$P\ \bar{1}$	*Cc*	$P2_1/c$	$R\ \bar{3}$	$R\ \bar{3}$
Crystal System	Triclinic	Monoclinic	Monoclinic	Trigonal	Trigonal
a (Å)	8.0331(14)	36.072(3)	11.205(4)	43.893(5)	44.2854(15)
b (Å)	11.6060(19)	11.1257(10)	34.385(11)	43.893(5)	44.2854(15)
c (Å)	17.834(3)	18.8177(17)	10.832(4)	11.6258(14)	11.4708(5)
α (°)	85.385(5)	90	90	90	90
β (°)	81.633(5)	114.556(3)	118.592(8)	90	90
γ (°)	89.097(5)	90	90	120	120
V ($Å^3$)	1639.7(5)	6868.9(11)	3664(2)	19397(5)	19482.5(16)
Z	1	4	2	9	9
D_{calc} (Mg/m^3)	1.294	1.317	1.329	1.432	1.426
Absorption coefficient (mm^{-1})	0.358	0.422	0.826	0.909	0.905
Data/restraints/parameter	5765 / 268 / 484	13998 / 925 / 1041	5427 / 236 / 518	7702 / 386 / 563	8213 / 489 / 623
Reflections collected	48287	103555	55504	127919	223507
Independent reflections	5765 [*R*(int) = 0.1510]	13998 [*R*(int) = 0.1434]	5427 [*R*(int) = 0.2453]	7702 [*R*(int) = 0.2372]	8213 [*R*(int) = 0.1369]
Goodness–of–fit (GOF) on F^2	1.021	1.018	1.009	1.007	1.017
Final *R* indices [I > 2sigma(I)]	*R*1 = 0.0641 w*R*2 = 0.1396	*R*1 = 0.0681 w*R*2 = 0.1659	*R*1 = 0.0610 w*R*2 = 0.1142	*R*1 = 0.0531 w*R*2 = 0.0962	*R*1 = 0.0474 w*R*2 = 0.1158
R indices (all data)	*R*1 = 0.1426 w*R*2 = 0.1757	*R*1 = 0.1416 w*R*2 = 0.2126	*R*1 = 0.1451 w*R*2 = 0.1473	*R*1 = 0.1209 w*R*2 = 0.1215	*R*1 = 0.0768 w*R*2 = 0.1333
Largest diff. peak and hole ($e.Å^{-3}$)	0.378 and –0.309	0.767 and –0.529	0.407 and –0.419	0.838 and –0.466	1.417 and –0.389
CCDC number	2404730	2404731	2404732	2404733	2404734

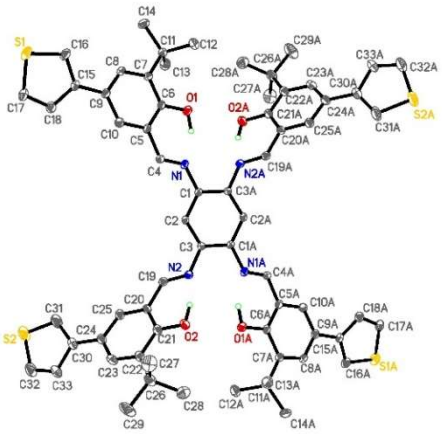

a

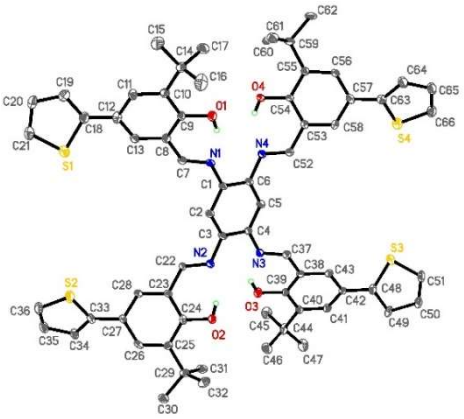

b

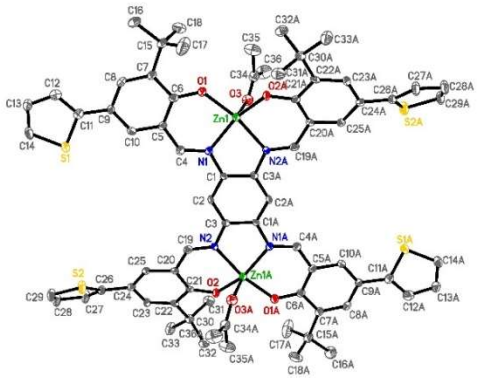

c

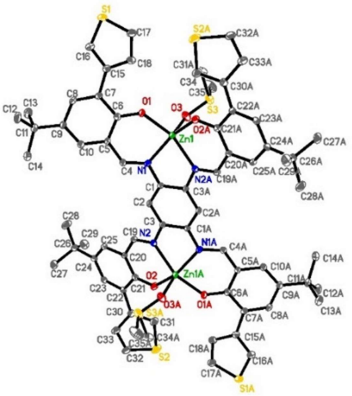

d

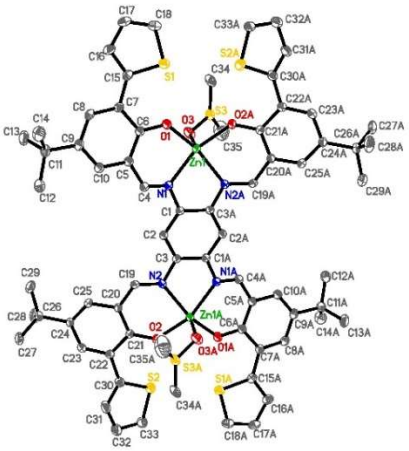

e

Figure S34: Molecular structures of tetra–Schiff bases 8 (a), 12 (b) and complexes 13 (c), 16 (d), 18 (e). Thermal ellipsoids represent 30% probability level. H, disordered atoms and solvent molecules are omitted for clarity.

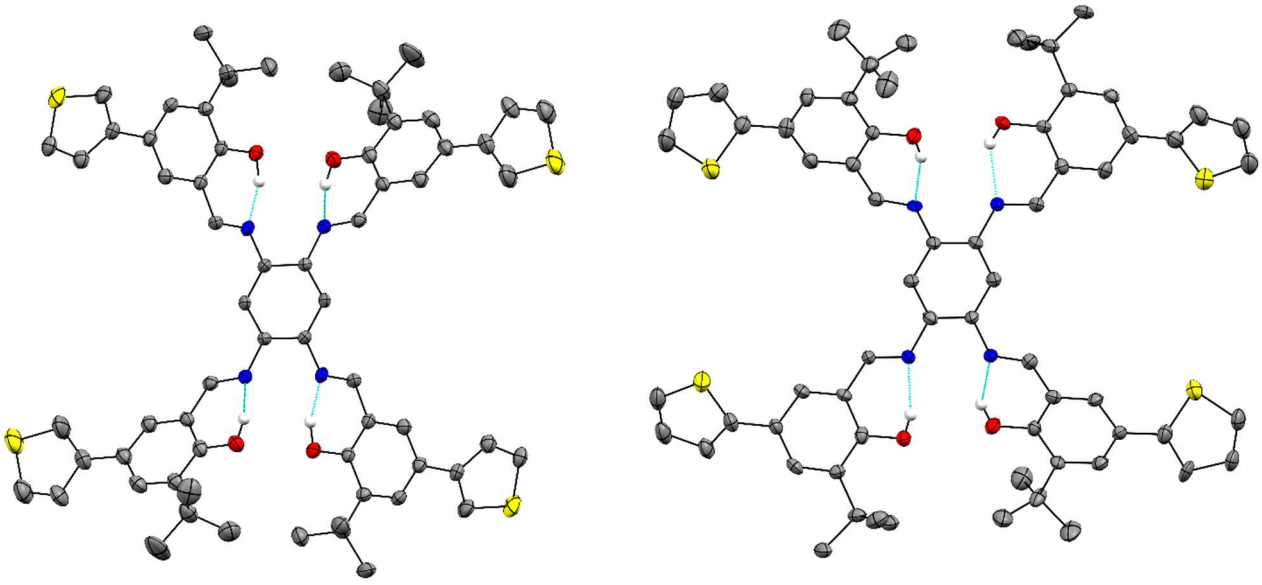

a b

Figure S35: Molecular views of ligands 8 (a) and 12 (b). Thermal ellipsoids represent 30% probability level. H atoms, except phenol OH, disordered atoms and solvent molecules are omitted for clarity. Intramolecular hydrogen bonding interactions are indicated by dashed lines.

Table S2. Selected bond lengths (Å) for ligands 8 and 12 and for complexes 13, 16 and 18.

Bond	Ligand **8**	Ligand **12**	Complex **13**	Complex **16**	Complex **18**
N1–C1	1.397(4)	1.412(10)	1.423(6)	1.417(5)	1.411(4)
N2–C3	1.416(4)	1.428(10)	1.400(6)	1.411(5)	1.409(4)
N3–C4 (**12**) / N1A–C1A	1.397(4)	1.440(10)	1.423(6)	1.417(5)	1.411(4)
N4–C6 (**12**) / N2A–C3A	1.416(4)	1.413(10)	1.400(6)	1.411(5)	1.409(4)
C1–C2	1.395(4)	1.404(12)	1.381(7)	1.390(6)	1.389(4)
C2–C3	1.386(4)	1.401(11)	1.389(7)	1.397(5)	1.391(4)
C3–C4 (**12**) / C3–C1A	1.407(4)	1.386(11)	1.422(7)	1.409(5)	1.411(4)
C4–C5 (**12**) / C1A–C2A	1.395(4)	1.392(12)	1.381(7)	1.390(6)	1.389(4)
C5–C6 (**12**) / C2A–C3A	1.386(4)	1.380(12)	1.389(7)	1.397(5)	1.391(4)
C6–C1 (**12**) / C3A–C1	1.407(4)	1.410(11)	1.422(7)	1.409(5)	1.411(4)
N1–C7 (**12**) / N1–C4	1.287(4)	1.273(11)	1.311(7)	1.298(5)	1.296(4)
N2–C22 (**12**) / N2–C19	1.271(4)	1.288(10)	1.296(7)	1.291(5)	1.288(4)
N3–C37 (**12**) / N1A–C4A	1.287(4)	1.287(10)	1.311(7)	1.298(5)	1.296(4)
N4–C52 (**12**) / N2A–C19A	1.271(4)	1.282(10)	1.296(7)	1.291(5)	1.288(4)
C9–O1 (**12**) / C6–O1	1.348(4)	1.353(10)	1.307(6)	1.303(5)	1.297(4)
C24–O2 (**12**) / C21–O2	1.353(4)	1.356(10)	1.306(6)	1.293(5)	1.296(4)
C39–O3 (**12**) / C6A–O1A	1.348(4)	1.362(9)	1.307(6)	1.303(5)	1.297(4)
C54–O4 (**12**) / C21A–O2A	1.353(4)	1.338(9)	1.306(6)	1.293(5)	1.296(4)
O1–Zn1/O1A–Zn1A	/	/	1.960(4)	1.971(3)	1.982(2)
O2A–Zn1/O2–Zn1A	/	/	1.971(4)	1.978(3)	1.980(2)
N1–Zn1/N1A–Zn1A	/	/	2.069(5)	2.088(3)	2.103(3)
N2A–Zn1/N2–Zn1A	/	/	2.065(4)	2.105(3)	2.120(3)
O3–Zn1/O3A–Zn1A	/	/	2.185(5)	2.072(3)	2.083(5)

Table S3. Selected bond angles (°) for ligands 8 and 12 and for complexes 13, 16 and 18.

angles	Ligand **8**	Ligand **12**	Complex **13**	Complex **16**	Complex **18**
C4–N1–C1/C7–N1–C1 (**12**)	125.9(3)	118.9(7)	120.9(5)	120.4(4)	120.4(3)
C19–N2–C3/C52–N4–C6 (**12**)	120.2(3)	118.4(7)	121.8(5)	120.5(4)	120.8(3)
C4A–N1A–C1A/C37–N3–C4 (**12**)	125.9(3)	117.5(7)	120.9(5)	120.4(4)	120.4(3)
C19A–N2A–C3A/C22–N2–C3 (**12**)	120.2(3)	119.1(7)	121.8(5)	120.5(4)	120.8(3)
N1–C1–C2/N1–C1–C2 (**12**)	125.3(3)	120.6(7)	125.7(5)	123.8(4)	124.2(3)
N1–C1–C3A/N1–C1–C6 (**12**)	115.6(3)	120.1(7)	115.1(5)	115.7(4)	115.7(3)
N2–C3–C2/N4–C6–C5 (**12**)	120.9(3)	123.2(7)	126.6(5)	125.7(4)	125.3(3)
N2–C3–C1A/N4–C6–C1 (**12**)	119.0(3)	117.8(7)	115.9(5)	115.5(3)	115.5(3)
N1–C4–C5/N1–C7–C8 (**12**)	120.6(3)	123.3(8)	126.2(5)	126.6(4)	125.9(3)
N2–C19–C20/N2–C22–C23 (**12**)	123.3(3)	123.2(7)	126.7(5)	126.1(4)	126.5(3)
N1A–C4A–C5A/N3–C37–C38 (**12**)	120.6(3)	123.0(8)	126.2(5)	126.6(4)	125.9(3)
N2A–C19A–C20A/N4–C52–C53 (**12**)	123.3(3)	122.3(8)	126.7(5)	126.1(4)	126.5(3)
N2A–C3A–C2A/N2–C3–C2 (**12**)	120.9(3)	121.1(7)	126.6(5)	125.7(4)	125.3(3)
N2A–C3A–C1/N2–C3–C4 (**12**)	119.0(3)	118.9(7)	115.9(5)	115.5(3)	115.5(3)
N1A–C1A–C2A/N3–C4–C5 (**12**)	125.3(3)	121.7(7)	125.7(5)	123.8(4)	124.2(3)
N1A–C1A–C3/N3–C4–C3 (**12**)	115.6(3)	119.0(7)	115.1(5)	115.7(4)	115.7(3)
C5–C6–O1/C8–C9–O1 (**12**)	120.7(3)	119.4(7)	123.0(5)	123.2(4)	124.1(3)
C7–C6–O1/C10–C9–O1 (**12**)	118.4(3)	119.2(7)	119.4(7)	120.7(4)	119.1(3)
C20–C21–O2/C23–C24–O2 (**12**)	119.9(3)	118.7(7)	122.6(5)	124.3(4)	123.6(3)
C22–C21–O2/C25–C24–O2 (**12**)	119.6(3)	119.9(8)	119.7(5)	119.4(4)	120.3(3)
C5A–C6A–O1A/C38–C39–O3 (**12**)	120.7(3)	120.1(7)	123.0(5)	123.2(4)	124.1(3)
C7A–C6A–O1A/C40–C39–O3 (**12**)	118.4(3)	119.2(7)	119.4(7)	120.7(4)	119.1(3)
C20A–C21A–O2A/C53–C54–O4 (**12**)	119.9(3)	120.2(7)	122.6(5)	124.3(4)	123.6(3)
C22A–C21A–O2A/C55–C54–O4 (**12**)	119.6(3)	119.3(7)	119.7(5)	119.4(4)	120.3(3)
O1–Zn1–O2A/O1A–Zn1A–O2	/	/	97.7(2)	96.6(1)	97.7(1)
O1–Zn1–N1/O1A–Zn1A–N1A	/	/	90.6(2)	88.8(1)	88.7(1)
O1–Zn1–O3/O1A–Zn1A–O3A	/	/	99.4(2)	98.0(1)	100.8(2)
O1–Zn1–N2A/O1A–Zn1A–N2	/	/	168.8(2)	157.1(1)	156.8(1)
O2A–Zn1–N2A/O2–Zn1A–N2	/	/	90.3(2)	88.3(2)	88.1(1)
O2A–Zn1–O3/O2–Zn1A–O3A	/	/	99.3(2)	98.6(1)	97.5(2)
O2A–Zn1–N1/O2–Zn1A–N1A	/	/	157.7(2)	154.2(1)	154.2(1)
N1–Zn1–N2A/N1A–Zn1A–N2	/	/	79.2(2)	77.8(1)	77.1(1)
N1–Zn1–O3/N1A–Zn1A–O3A	/	/	99.8(2)	105.6(1)	105.9(2)
N2A–Zn1–O3/N2–Zn1A–O3A	/	/	87.0(2)	103.4(1)	100.7(2)

Table S4. Torsion angles (°) for ligands 8 and 12 and for complexes 13, 16 and 18.

Torsion angles	Ligand **8**	Ligand **12**	Complex **13**	Complex **16**	Complex **18**
C4–N1–C1–C2 / C7–N1–C1–C2 (**12**)	16.4(5)	38.2(12)	10.9(9)	25.3(6)	22.6(5)
C19–N2–C3–C2 / C22–N2–C3–C2 (**12**)	53.5(4)	35.1(12)	2.3(9)	12.1(6)	14.9(5)
C4A–N1A–C1A–C2A / C37–N3–C4–C5 (**12**)	16.4(5)	36.9(12)	10.9(9)	25.3(6)	22.6(5)
C19A–N2A–C3A–C2A / C52–N4–C6–C5 (**12**)	53.5(4)	33.8(13)	2.3(9)	12.1(6)	14.9(5)

Table S5. Hydrogen bonds (Å and °) for ligand 8.

D–H...A	d(D–H)	d(H...A)	d(D...A)	<(DHA)
O1–H1A...N1	0.94(4)	1.72(4)	2.514(4)	156(4)
O1–H1A...N2A	0.94(4)	2.76(4)	3.385(4)	133(3)
O2–H2A...N2	0.93(4)	1.75(4)	2.610(4)	158(3)

Symmetry transformations used to generate equivalent atoms: –x+2,–y+2,–z+1

Table S6. Hydrogen bonds (Å and °) for ligand 12.

D–H...A	d(D–H)	d(H...A)	d(D...A)	<(DHA)
O1–H1...N1	0.81(4)	1.85(6)	2.612(9)	157(10)
O2–H2...N2	0.81(4)	1.87(6)	2.609(10)	152(9)
O3–H3...N3	0.81(4)	1.93(7)	2.610(10)	141(9)
O4–H4...N4	0.79(5)	1.96(7)	2.599(10)	138(9)

V. References

1. SAINT, *Program for data reduction (Bruker-AXS)*.
2. SADABS, *Program for data correction (Bruker-AXS)*.
3. G. M. Sheldrick, ShelXT, *Acta Crystallogr. Sect. A*, 2015, **71**, 3-8.
4. G. M. Sheldrick, ShelXL, *Acta Crystallogr. Sect. C*, 2015, **71**, 3-8.
5. A. L. Spek, *Acta Crystallogr. Sect C*, 2015, **71**, 9-18.
6. V. Ramakrishna and N. D. Reddy, *Dalton Trans.*, 2017, **46**, 8598-8610.
7. A. Pietrangelo, B. N. Boden, M. J. MacLachlan and M. O. Wolf, *Can. J. Chem.*, 2009, **87**, 314-320.
8. A. Gillet, S. Cher, M. Tasse, T. Blon, S. Alves, G. Izzet, B. Chaudret, A. Proust, P. Demont, F. Volatron and S. Tricard, *Nanoscale Horiz.*, 2021, **6**, 271-276.
9. N. Marchenko, D. Martin, A. Pham, S. Abid, E. Cretal, A. Ibarra, D. Lagarde, M. Tassé, J. Bonvoisin, G. Rapenne, J. Grisolia, C. Kammerer and S. Tricard, *Mater. Horiz.*, 2025, **12**, 3429-3435.